

Durham Research Online

Deposited in DRO:

26 September 2016

Version of attached file:

Published Version

Peer-review status of attached file:

Peer-reviewed

Citation for published item:

de Lucas, Miguel and Pu, Li and Turco, Gina Marie and Gaudinier, Allie and Marao, Ana Karina and Hiroshima, Hirofumi and Kim, Dahae and Ron, Mily and Sugimoto, Keiko and Roudier, Francois M. and Brady, Siobhan M. (2016) 'Transcriptional regulation of Arabidopsis Polycomb Repressive Complex 2 coordinates cell type proliferation and differentiation.', *Plant cell*, 28 (10). pp. 2616-2631.

Further information on publisher's website:

<http://dx.doi.org/10.1105/tpc.15.00744>

Publisher's copyright statement:

Copyright American Society of Plant Biologists.

Additional information:

Use policy

The full-text may be used and/or reproduced, and given to third parties in any format or medium, without prior permission or charge, for personal research or study, educational, or not-for-profit purposes provided that:

- a full bibliographic reference is made to the original source
- a [link](#) is made to the metadata record in DRO
- the full-text is not changed in any way

The full-text must not be sold in any format or medium without the formal permission of the copyright holders.

Please consult the [full DRO policy](#) for further details.

RESEARCH ARTICLE

Transcriptional Regulation of Arabidopsis Polycomb Repressive Complex 2 Coordinates Cell Type Proliferation and Differentiation

Miguel de Lucas^{1*}, Li Pu¹, Gina Turco¹, Allison Gaudinier¹, Ana Karina Morao², Hirofumi Harashima³, Dahae Kim¹, Mily Ron¹, Keiko Sugimoto³, Francois Roudier², Siobhan M. Brady¹

¹Department of Plant Biology and Genome Center, University of California, Davis, Davis, CA 95616, USA

²Institut de Biologie de l'Ecole Normale Supérieure (IBENS), Centre National de la Recherche Scientifique (CNRS) Unité Mixte de Recherche (UMR) 8197 and Institut National de la Santé et de la Recherche Médicale (INSERM) U1024, Paris, France.

³RIKEN Center for Sustainable Resource Science, 1-7-22 Suehiro, Tsurumi, Yokohama, 230-0045 Japan

*Current address: School of Biological and Biomedical Sciences, Durham University, Durham, DH1 3LE, UK.

Corresponding Author: Siobhan Brady: sbrady@ucdavis.edu

Short title: A multi-tier PRC2 regulatory network

One-sentence summary: Chromatin-modifying PRC2 subunits were shown to regulate root vascular development, and their upstream regulators were identified and shown to control the expression of PRC2 downstream targets.

The authors responsible for distribution of materials integral to the findings presented in this article in accordance with the policy described in the Instructions for Authors (www.plantcell.org) are: Siobhan M. Brady (sbrady@ucdavis.edu) and Miguel de Lucas (miguel.de-lucas@durham.ac.uk).

ABSTRACT

Spatiotemporal regulation of transcription is fine-tuned at multiple levels, including chromatin compaction. Polycomb Repressive Complex 2 (PRC2) catalyzes the trimethylation of Histone 3 at lysine 27 (H3K27me3), which is the hallmark of a repressive chromatin state. Multiple PRC2 complexes have been reported in *Arabidopsis thaliana* to control the expression of genes involved in developmental transitions and maintenance of organ identity. Here, we show that PRC2 member genes display complex spatiotemporal gene expression patterns and function in root meristem and vascular cell proliferation and specification. Furthermore, PRC2 gene expression patterns correspond with vascular and non-vascular tissue-specific H3K27me3-marked genes. This tissue-specific repression via H3K27me3 regulates the balance between cell proliferation and differentiation. Using enhanced yeast-one-hybrid analysis, upstream regulators of the PRC2 member genes are identified, and genetic analysis demonstrates that transcriptional regulation of some PRC2 genes plays an important role in determining PRC2 spatiotemporal activity within a developing organ.

INTRODUCTION

The formation of new organs involves transcriptional reprogramming of pluripotent stem cells in order to give rise to different cell types. This temporal and spatial regulation of gene expression are regulated at multiple levels, including chromatin compaction via histone post-translational modifications, a general mechanism by which promoter accessibility is regulated to enable interaction with transcription factors and RNA polymerase machinery. Despite the extensive chromatin modification data generated in recent years, few studies have evaluated the transcriptional regulation of chromatin modifiers themselves. Polycomb Repressive Complex 2 (PRC2) catalyzes the trimethylation of Histone 3 protein at the lysine 27 position (H3K27me3), the hallmark of a silent chromatin state that is correlated with gene repression and its maintenance across cell division.

PRC2 structure is highly conserved, with four core sub-units conventionally named after their homologs in *Drosophila*, including an Enhancer of zeste (E(z)) catalytic SET domain-containing protein, an Extra sex combs (Esc) protein, a nucleosome remodeling factor WD40-containing protein (Nurf55), and a Suppressor of zeste 12 zinc finger protein in a stoichiometric ratio of 1:1:1:1 (Ciferri et al., 2012). However, the number of genes that encode each sub-unit varies between species (Mozgová and Hennig, 2015). The *Drosophila* genome has been described as containing a single gene for each subunit, which consequently constitute a single complex. However, two copies of the Extra sex combs gene, *ESC* and *ESCL*, have been reported (Ohno et al., 2008). In mouse and human there are two copies of the E(z) gene – *EZH1* and *EZH2* (Ciferri et al., 2012; Margueron et al., 2008). In addition, distinct isoforms of Esc have been reported in human (Mozgová and Hennig, 2015; Kuzmichev et al., 2005). The *Arabidopsis thaliana* genome encodes three homologous genes for the E(z) methyltransferase subunit, *MEDEA* (*MEA*), *CURLY LEAF* (*CLF*) and *SWINGER* (*SWN*), one for Esc, *FERTILIZATION INDEPENDENT ENDOSPERM* (*FIE*), five WD40-containing protein genes, *MULTICOPY SUPPRESSOR OF IRA1-5* (*MSI1–5*), and three Su(z)12, *FERTILIZATION INDEPENDENT SEED2* (*FIS2*), *EMBRYONIC FLOWER2* (*EMF2*) and *VERNALIZATION2* (*VRN2*). Together, these subunits have been reported to form three PRC2 complexes, with the methyltransferases acting partially redundantly (Ohno et al., 2008; Chanvivattana et al., 2004; Bemmer and Grossniklaus, 2012). Several thousand genes are regulated by PRC2, and distinct complexes have been reported to regulate the expression of genes involved in developmental transitions (Bouyer et al., 2011; Zhang et al., 2007a). The FIS2 complex

comprises FIS2, FIE, MEA, and MSI1 and functions in the female gametophyte and endosperm to repress *PHERES* (Köhler et al., 2005). The expression of key regulators of the vegetative-to-reproductive transition, such as *LEAFY* and *AGAMOUS*, are regulated by the EMF2 complex (EMF2, FIE, CLF or SWN and MSI1) (Kinoshita et al., 2001). A third complex (VRN2), which comprises VRN2, FIE, CLF or SWN and MSI1, represses *FLOWERING LOCUS C* to accelerate flowering in response to cold (De Lucia et al., 2008).

The regulatory mechanisms that determine which of these complexes are able to act at these specific developmental transitions are unclear. Here, we describe spatiotemporal transcriptional regulation of PRC2 genes in the Arabidopsis root and characterize their function in cellular patterning, proliferation and differentiation. The Arabidopsis root has a simple structural and functional organization consisting of concentric cylinders of cell layers with radial symmetry. Briefly, root growth and development rely on the continuous activity of the apical meristem, where multipotent stem cells surround a small population of centrally located organizing cells, the quiescent center (Scheres, 2007; Terpstra and Heidstra, 2009). Owing to a stereotypical division pattern, stem cells, depending on their position, give rise to different cell files in which the spatial relationship of cells in a file reflects their age and differentiation status (Benfey and scheres, 2000; Dolan et al., 1993). The epidermis is present on the outside and surrounds the cortex, endodermis and pericycle layers. The internal vascular cylinder consists of xylem, phloem and procambium tissues.

Here we demonstrate that PRC2 controls root meristem development and regulates vascular cell proliferation in the maturation zone. Distinct suites of genes are marked by H3K27me3 in vascular and non-vascular cells to regulate the balance between cellular proliferation and differentiation. Dozens of transcription factors bind to the promoters of genes that encode PRC2 subunits and regulate their expression in Arabidopsis. Together, this multilayered regulatory network provides key insights into the varied means by which gene expression is regulated to ensure appropriate morphogenesis and functioning of a plant organ.

RESULTS

PRC2 subunits show regulated transcript and protein abundance in the Arabidopsis root

A variety of PRC2 complexes act at distinct developmental transitions during the Arabidopsis life cycle (Kinoshita et al., 2001; Chanvivattana et al., 2004). Spatial and

temporal gene expression data in the Arabidopsis root (Supplemental Figure 1) suggest that transcriptional regulation may be an important component in determining the presence of specific PRC2 genes in different cell types. SWN, EMF2 and VRN2 proteins have previously been reported in the root meristem and in root hairs (Ikeuchi et al., 2015). To further validate the spatiotemporal expression pattern of PRC2 subunits, we generated transcriptional fusions for each PRC2 gene (Figure 1A-H) and studied the respective reporter expression pattern within the root. *MEA* was not expressed within the root, while *FIS2* was expressed in the columella (Figure 1C,F). The potential promoter regions of most subunits drove strong expression in all cell types in the meristematic zone that then became preferentially detectable in the vascular cylinder in the elongation and maturation zones (Figure 1A-H). *CLF* in particular showed enrichment in the root vasculature in both the meristem and maturation region of the root, and this was corroborated by an *in situ* hybridization with a probe to the *CLF* transcript (Figure 1E, Supplemental Figure 2D). Translational fusions, for all but *FIS2*, were then used to determine if further regulatory mechanisms might also affect PRC2 protein abundance. SWN protein abundance was enriched within the epidermal and ground tissue layers in the meristem (Figure 2C). The CLF protein, in a complemented *clf-29* mutant background, was found in the root meristem and enriched in the vascular tissue in the maturation zone (Figure 2E, Supplemental Figure 3B). CLF protein in a complemented *clf-28swn-7* background shows the same enrichment patterns (Supplemental Figure 2E). Within the root meristem and elongation zone, SWN, EMF2, VRN2 and FIE (in a complemented *fie-1* mutant background) proteins are present (Figure 2A, B, C, F) (Ikeuchi et al., 2015; Kinoshita et al., 2001). In the differentiation zone, however, SWN, EMF2, VRN2 and FIE proteins are present primarily in vasculature (Figure 2A, B, C, F), although VRN2, EMF2 and SWN protein has also been reported in root hairs (Ikeuchi et al., 2015).

PRC2 activity is required for proper root development

The expression and protein abundance patterns of PRC2 genes suggested that PRC2 might influence cell patterning or specification in the Arabidopsis root. Since the MEA protein is not found within the Arabidopsis root, CLF and SWN are the only methyltransferases that are candidate regulators of root development. To test the consequences of loss of PRC2 in root cell specification and patterning, we analyzed the phenotypes of *clf-28 swn-7*, which produce viable embryos with PRC2 function eliminated after germination. In agreement with (Lafos et al., 2011), the *clf-28 swn-7* mutants showed a complete loss of H3K27me3 deposition, as revealed using whole mount

immunocytochemistry (Figure 3A,B). However, both the *clf-29* and *swn-7* single mutants show nuclear H3K27me3 (Supplemental Figure 3, 4), suggesting that these proteins have partially redundant functions. Analysis of the single and double mutant combinations of CLF and SWN demonstrated that they interact genetically. The *swn-7* allele has a shorter root with no difference in meristem size, while *clf-29* shows no difference in root length but has a significant increase in the number of cells in the root meristem, as previously reported (Figure 3J-K) (Aichinger et al., 2011). The roots of *clf-28 swn-7* double mutants are shorter than those of wild type, with a small meristem containing fewer cells (Figure 3C-D,J-K), as does a *clf-29 swn-7* double mutant (Supplemental Figure 5C-D). Although no defects in radial cell patterning were observed, the number of cells in the vascular cylinder was significantly increased (Figure 3E-G,I Supplemental Figure 5A). In striking similarity with the *clf-28 swn-7* phenotype, the *fie* mutant (Bouyer et al., 2011) displayed a smaller meristem with fewer cells (Supplemental Figure 5B) in addition to a large increase in the number of cells within the vascular cylinder (Figure 3G). This increase in vascular cell number was characterized by an increase in protoxylem and metaxylem cells (Figure 3L-M).

Although there are several MSI1 homologs, immunopurification experiments determined that MSI1 is the primary WD40 protein required for PRC2 activity in Arabidopsis (Derkacheva et al., 2013). It should be noted however, that MSI1 is also a member of other chromatin modifying complexes (Jullien et al., 2008). Given the vascular phenotypes of mutations in other PRC2 genes and in order to circumvent the female gametophytic lethality of *msi1* mutants (Köhler et al., 2003), we generated a transgenic line that expressed an artificial miRNA (amiRNA) targeting *MSI1* under the *WOODEN LEG (WOL)* promoter (*WOL_{pro}:amiRNA_MSI1*) (Inoue et al., 2001), the expression of which is restricted to the vascular cylinder of the root. To validate *MSI1* silencing, we introduced the transgene into a line containing *MSI1_{pro}:MSI1:GFP* (Figure 3N,O). We tested for changes in H3K27me3 deposition in *MSI1* silenced lines and observed a reduction specifically in the vascular cylinder (Supplemental Figure 6). The *MSI1_{pro}:MSI1:GFP* signal was undetectable in the *WOL_{pro}:amiRNA_MSI1* vascular cylinder (Figure 3I-J). Silencing of *MSI1* in the vascular cylinder was sufficient to decrease overall root growth (Figure 3P,Q), with fewer cells in the meristem, similar to the phenotypes observed in *clf-28 swn-7* and *fie*. However, in contrast to *clf-28 swn-7* and *fie*, which showed an increase in cell number, a statistically significant decrease in vascular cell number was observed (Figure 3G,M).

Taken together, our results indicate that PRC2 regulates both root meristem cell number and vascular cell proliferation.

Genes specifically marked by H3K27me3 in vascular and non-vascular tissue

Many genes marked by H3K27me3 have distinct cell type or tissue-specific expression patterns (Turck et al., 2007; Zhang et al., 2007a; Deal and Henikoff, 2010; Lafos et al., 2011) and the data presented above suggested that PRC2 likely regulates the expression of many genes in the vasculature as well as in other cell types within the root. In order to identify the genes specifically marked by H3K27me3 in the vascular tissue relative to the whole root, we carried out fluorescent activated cell sorting using the WOL_{pro}:GFP marker line (Birnbaum et al., 2003) (Supplemental Figure 7A-C) coupled with ChIP-seq using an antibody specific for H3K27me3. As a control, we also carried out ChIP-seq with an antibody specific for H3K4me3, a chromatin modification associated with expressed genes. As expected from previous reports (Zhang et al., 2007b; Roudier et al., 2011), genes marked with H3K27me3 showed lower expression relative to genes with H3K4me3 (Figure 4A). Comparison between the list of genes marked by H3K27me3 in the WOL_{pro} population and in the root protoplast population (Figure 4B) identified 130 genomic regions marked by H3K27me3 specifically in the vascular cylinder (Figure 4B). In comparison, 2859 genes were specifically enriched in H3K27me3 outside of the vascular tissue (Supplemental Data Set 1). To identify biological processes over-represented in H3K27me3-marked regions associated with the WOL_{pro}:GFP sorted population relative to the whole root population, we carried out Gene Ontology (GO) enrichment analysis (Du et al., 2010). Among these lists of H3K27me3-marked genes, 113 and 82 GO categories were significantly enriched in the WOL_{pro}:GFP population and the whole root population, respectively (Supplemental Data Set 1). 37 GO terms were enriched only in the WOL_{pro}:GFP population, while 6 GO terms were enriched only in the whole root population and thus may represent non-vascular-specific GO terms, although they were not significantly under-represented within the WOL_{pro}:GFP population (Supplemental Figure 6D, Supplemental Data Set 1). The set of non-vascular-specific GO terms are consistent with repression of biological processes associated with vascular development and include axis specification, adaxial/abaxial pattern formation, meristem maintenance, phloem or xylem histogenesis, xylem development, and cell wall organization or biogenesis. In the WOL_{pro}:GFP -specific samples, H3K27me3-marked genes were enriched for floral development, gibberellin-related processes and terpenoid metabolism, suggesting differential regulation of these pathways within vascular cells.

Functional importance of tissue-specific PRC2-mediated repression

In order to identify H3K27me3-marked genes that are transcriptionally repressed in the vascular cylinder or in non-vascular cells, we further restricted the lists of H3K27me3-marked genes using cell type-specific gene expression data (Brady et al., 2007). The auxin response factor *ARF17* is marked specifically by H3K27me3 in vascular tissue and is not expressed in the vascular cylinder. This non-vascular expression pattern was confirmed using a transcriptional fusion in which GFP is expressed under the *ARF17* promoter (Figure 4C) (Ciferri et al., 2012; Okushima, 2005). Conversely, *VND7*, a well-described regulator of vascular development, was marked by H3K27me3 in non-vascular cells and is specifically expressed in vascular tissue, as confirmed by the use of a promoter:reporter (YFP) fusion (Mozgová and Hennig, 2015; Yamaguchi et al., 2010) (Figure 4E-F).

In order to determine the functional importance of PRC2-mediated repression, we sought to over-ride/bypass the silencing in the vasculature presumably conferred by the PRC2 by expressing *ARF17* under the control of a β -estradiol-inducible promoter (Ohno et al., 2008; Coego et al., 2014). This is a similar approach to one described for *AGAMOUS*, a PRC2 target gene (Ciferri et al., 2012; Sieburth and Meyerowitz, 1997; Margueron et al., 2008) and other target genes (Mozgová and Hennig, 2015; Ikeuchi et al., 2015; Kuzmichev et al., 2005). The constitutive induction of *ARF17* in the root caused a loss of organization of the root pattern, with frequent observations of ectopic cell proliferation (Figure 4G-J and Supplemental Figure 3A). In contrast, ectopic expression of *VND7* with the β -estradiol-inducible promoter induced ectopic xylem cell differentiation, as has been previously reported (Ohno et al., 2008; Kubo, 2005; Chanvivattana et al., 2004; Bemer and Grossniklaus, 2012) (Figure 4E-F, K-L). Thus, these PRC2-target genes regulate the correct balance between cell proliferation and cell differentiation.

Transcriptional regulation of PRC2 core components in the Arabidopsis root

The differential spatiotemporal expression patterns of PRC2 genes suggest a regulatory role for transcription factors in determining this specificity. We thus utilized the 5' flanking regions upstream of the translational start site of PRC2 genes in the synthesis of the transcriptional fusions as bait in an enhanced yeast one-hybrid assay (Bouyer et al., 2011; Lee et al., 2006; Zhang et al., 2007a; Brady et al., 2011; Taylor-Teeple et al., 2015). In order to focus on the vascular-specific regulation of these genes, we screened the promoters against a set of root vascular-expressed transcription factors (Köhler et al.,

2005; Gaudinier et al., 2011) (Kinoshita et al., 2001; Reece-Hoyes et al., 2011) (Supplemental Data Set 2). In total, 101 transcription factors (out of 653) interacted with these potential promoters (Figure 5), with ten TF families over-represented (C2H2, bHLH, Homeobox, MYB, AP2-EREBP, WRKY, GRAS, bZIP, C2C2-Dof, and ARF; p-value < 0.01). In order to validate these transcription factor-promoter interactions *in planta*, we performed two types of assays. Transcription factors were overexpressed using a β -estradiol-inducible system (De Lucia et al., 2008; Coego et al., 2014) and expression of the respective target gene was measured 24 hours after induction (Supplemental Data Set 3). In addition, myc-tagged transcription factors were assessed for their ability to drive expression of the GUS reporter gene fused to the target promoter in *Nicotiana benthamiana* leaves (Supplemental Data Set 3). Altogether, 71 of the 101 transcription factors in the network were tested in these *in planta* assays and a total of 63 interactions were successfully validated *in planta* (Supplemental Data Set 3, Figure 5, Supplemental Figure 8). We hypothesize that these transcription factors represent an important upstream regulatory component of PRC2 gene expression. We next postulated that distinct TFs could control the expression of PRC2 genes in different cell types. To address this question, we investigated the co-expression patterns between each TF and their target gene using spatial root transcriptome data (Scheres, 2007; Brady et al., 2007; Terpstra and Heidstra, 2009) (Supplemental Figure 7). A total of 9 TF-promoter interactions were significantly and highly correlated across cell types ($r \geq \pm 0.6$) (Supplemental Data Set 3). Together, our data demonstrate that a diverse set of transcription factors is sufficient to regulate PRC2 expression *in planta*, along with other factors including the regulation of the chromatin environment, which likely act in a combinatorial regulatory code to specify PRC2 gene expression.

Transcriptional Regulation of PRC2 Components Contributes to PRC2-Mediated Regulation of Cell Proliferation and Differentiation

In order to determine the functional contribution of transcription factors controlling PRC2 gene expression that in turn regulate the expression of PRC2 target genes, we focused on the DOF6 transcription factor, which activates *CLF* expression both in transient and estradiol induction assays (Supplemental Data Set 1 and 3). The induction of *DOF6* causes severe inhibition of root growth but increases the number of cells in the meristem (Figure 6A, Supplemental Figure 2A-B). Both *DOF6* and *CLF* are also both expressed in root vascular tissue, further supporting the possibility of this regulatory interaction *in planta* (Rueda-Romero et al., 2012) (Figure 1E and Supplemental Figure 2C-D). Since DOF6 is

sufficient to increase *CLF* expression (Figure 6C), our hypothesis was that *DOF6* overexpression could lead to an increase in *CLF* expression in non-vascular tissue, which in turn could result in an increase in PRC2 activity in these cell types, as determined by measuring gene expression and corresponding H3K27me3 levels. Our H3K27me3 ChIP-seq data demonstrate that *ARF17* is a vascular-specific target of PRC2, and the transcriptional fusion data demonstrate that *ARF17* is only expressed outside of the vasculature (Figure 4C, Supplemental Data Set 1). *ARF17* is a target of PRC2 complexes containing CLF but not SWN based on the increase in gene expression in *clf-29* versus *swn-7* mutants (Figure 6B). Furthermore, overexpression of a miRNA160-resistant version of *ARF17* results in prominent vegetative and floral defects similar to those observed in *clf-29*, including upward curling of leaf margins, reduced plant size, accelerated flowering time, and reduced fertility (Kinoshita et al., 2001; Mallory, 2005; Chanvivattana et al., 2004). We thus chose *ARF17* as a candidate to explore the influence of PRC2 gene expression manipulation on its target gene (*ARF17*) expression.

Over-expression of *DOF6* led to increased expression of *CLF* concomitantly with a decrease in *ARF17* expression (Figure 6C). This decrease in *ARF17* expression is dependent on CLF, as shown in the *DOF6* estradiol-inducible line in the *clf-29* mutant background (Figure 6E). Furthermore, the domain of *ARF17* expression expanded to the vascular cylinder in a *clf-29* mutant background (Figure 6F), demonstrating that CLF is sufficient to regulate the spatial expression pattern of *ARF17*. Finally, H3K27me3 of *ARF17* is increased upon *DOF6* induction (Figure 6D), demonstrating that *DOF6* increases the expression of *CLF* and, in turn, CLF regulates the expression of the target gene *ARF17* through changes in H3K27me3. An additional influence of CLF was observed with respect to the regulation of root length. When the *clf-29* mutation was introduced into the *DOF6* estradiol-inducible line, upon estradiol induction, no influence on root length was observed. Thus, we identified transcription factors that are sufficient to control the expression of PRC2 genes in the root, and we demonstrated that altered expression of these transcription factors can disrupt the expression of a PRC2 subunit gene in addition to the levels of H3K27me3 and the corresponding expression of its target gene.

DISCUSSION

A Multi-tiered Regulatory Network for Gene Expression

We systematically characterized the regulation of PRC2 gene expression at cell type-resolution using Arabidopsis roots as a model system. We showed that there are distinct spatial and temporal transcript accumulation patterns for PRC2 components. The heterologous (yeast/*N. benthamiana*) and *in vivo* (Arabidopsis) approaches we employed revealed a transcriptional network that controls PRC2 gene expression in the Arabidopsis root. Altogether, our data provide evidence that transcriptional control of the PRC2 component *CLF*, and likely of other PRC2 components, plays an important role in determining H3K27me3 levels and the corresponding expression of H3K27me3 targets in a spatiotemporal manner. This regulation is likely complemented by other previously described modes of regulation in Arabidopsis, including *cis*-regulatory regions similar to the Polycomb Repressive Element in *Drosophila* (Ikeuchi et al., 2015; Deng et al., 2013), long non-coding RNAs, and protein–protein interactions via Polycomb Repressive Complex 1 (PRC1) and PRC1-like genes to determine target specificity and chromatin compaction (Ikeuchi et al., 2015; Margueron and Reinberg, 2011).

Further dissection of these distinct tiers of this regulatory network is needed. At the upper level of the network, the correlation of expression between transcription factors and their target PRC2 genes (Gu et al., 2014; Brady et al., 2007) suggests that distinct groups of transcription factors regulate the expression of these genes in space, in time, or in both space and time (Supplemental Data Set 1). At the second tier of the network, analyses of PRC2 gene mutants demonstrated that *CLF*, *SWN* and *FIE*, key components of PRC2, functionally regulate root meristem and vascular development, likely at the level of cell division. Additionally, the translational fusion patterns suggest that only a restricted number of complexes can form at a particular cell type or temporal stage of development. It will be interesting in the future to determine if the cell type- or tissue-specific expression patterns of *CLF* or *SWN* are necessary to regulate the H3K27me3 of distinct suites of genes. In addition, in proximal meristematic vascular tissue, *CLF* and *SWN* protein were both present. The mechanism by which different complexes form and how the affinity for different targets is determined remain to be described. At the final tier of the network, whether distinct PRC2 complexes regulate distinct groups of genes within the root meristem remains to be determined. However, our data showing vascular-specific H3K27me3 and silenced genes provide proof of such suites of genes at the level of individual tissues.

Regulation of Cell Proliferation and Differentiation during Arabidopsis Root Development

In plants, PRC2 proteins maintain organ and cell-type identity, regulate developmental transitions, repress cell proliferation (Lafos et al., 2011; Hennig and Derkacheva, 2009) and regulate totipotency (Aichinger et al., 2009; He et al., 2012). Here, we report two additional functions of PRC2 in post-embryonic development: the regulation of cell proliferation in vascular tissue, and the appropriate execution of xylem cell differentiation (Figure 3E-G; L-M). In the developing root, procambium cells are the stem cell source responsible for vascular cell types and secondary growth (Bouyer et al., 2011; Mahonen, 2006; 2000; De Rybel et al., 2014). Procambium cells proliferate and can undergo differentiation into either xylem cells or phloem cells depending on positional cues (Derkacheva et al., 2013; Fisher and Turner, 2007; Etchells et al., 2013; Etchells and Turner, 2010). The vascular proliferation phenotype of the *clf-28 swn-7* mutant suggests that PRC2 represses division of the procambium cell population. *CLF* and *SWN* are not responsible for initiating division of these cells, but rather, when the appropriate number of cells has been produced, PRC2 activity likely negatively influences chromatin accessibility for transcription factors such as *ARF17* in addition to cell cycle regulators. The over-proliferation phenotype of the *ARF17* over-expressor and its similarity to the phenotype of the *clf28swn7* mutant suggest that *ARF17* may be such a cell cycle regulator. The lack of a vascular phenotype in the *clf29* mutant implies that cell proliferation is likely also controlled by other *SWN*-dependent H3K27me3 targets. On the other hand, the *fie-042* ectopic xylem cell phenotype, the tissue-specific *VND7* H3K27me3 deposition pattern, and the finding that over-riding this repression through ectopic expression results in ectopic xylem differentiation suggest that tissue-specific PRC2 activity ensures the appropriate execution of the xylem cell differentiation program.

Knockdown of *MSI1* in the vascular tissue resulted in a very different phenotype relative to that observed in mutants of other PRC2 subunits. In the vascular cylinder, the planes of division were altered suggesting that this particular gene likely plays a role in procambium cell patterning. Interestingly, *WOL_{pro}:amiRNA_MSI1* expression resulted in a short root phenotype despite being only driven in the vascular cylinder. This could be due to cell non-autonomous effects, defects in vascular development influencing overall growth, or a defect in the vascular initial cells, which determine quiescent cell identity. *MSI1* is a member of other chromatin modifying complexes including the CAF1 complex, which is associated with nucleosome deposition for chromatin assembly and histone deacetylation (Jullien et al., 2008; Hennig et al., 2003). Thus, the phenotypes observed may reflect

developmental decisions occurring during early root patterning or independent of PRC2 activity.

A Comparative Perspective on PRC2 Function in Plants and Animals

In animal embryonic stem cells and outside of the embryo, PRC2 is required for the maintenance of differentiation potential (Köhler et al., 2003; Laugesen and Helin, 2014). Mutations in PRC2 subunits can either delay differentiation of myogenic or neurogenic cell types or precociously advance the differentiation of particular cell types in addition to preserving the appropriate cell identity (Inoue et al., 2001; Stojic et al., 2011; Pasini et al., 2007; Hirabayashi et al., 2009; Fasano et al., 2007; Sher et al., 2008; Aldiri and Vetter, 2009). In contrast, in the plant procambial stem cell population, PRC2 regulates self-renewal capabilities (Turck et al., 2007; Laugesen and Helin, 2014; Zhang et al., 2007a; Deal and Henikoff, 2010; Lafos et al., 2011). Our data also demonstrate that in root cells, PRC2 ensures the correct cell type-specific differentiation state through spatially repressing the expression of cell type-specific developmental regulators (VND7). Thus, in plants, PRC2 regulates self-renewal of the procambial stem cell population in addition to cell differentiation.

Uncontrolled abundance, increased activity, or loss of function of PRC2 components can lead to disease (Birnbaum et al., 2003; Bracken et al., 2003; Kleer et al., 2003; Takawa et al., 2011; Varambally et al., 2002; Wagener et al., 2010). Thus, our findings indicate that transcription factors may be an important component in determining PRC2 gene expression in animals, and through this mechanism, the repression of their targets. Furthermore, in cases where multiple genes have been found to encode a single PRC2 subunit, the expression patterns of these subunits and their upstream regulation should be systematically explored. Epigenetic abnormalities are common in human cancer and play a key role in tumor progression, and hence, significant efforts have focused on developing inhibitors of these PRC2 proteins to treat disease (Zhang et al., 2007b; Helin and Dhanak, 2013; Roudier et al., 2011). The characterization of cell type or tissue-specific regulation of PRC2 gene expression may provide an additional mode by which the negative effects caused by PRC2 misregulation could be abrogated.

METHODS

Plant material

All transgenic *Arabidopsis thaliana* plants and mutants are in the Col-0 background except for the VRN2_{pro}:VRN2:GUS line (kindly provided by Caroline Dean), which is in the Ler

background, as is the FIEpro:FIE:GFP line (Kinoshita et al., 2001). The *clf-28 swn-7* (SALK_139371, SALK_109121), *clf-29* (SALK_021003), *swn-7* (SALK_109121), and *fie* (SALK_042962) (Du et al., 2010; Bouyer et al., 2011) mutants were kindly provided by François Roudier and Daniel Bouyer, respectively. The DOF6 β -estradiol inducible, VND7 and ARF17 transcriptional and FIE in *fie-1*, SWN and MEA in *mea-3* translational fusions have been described elsewhere (Brady et al., 2007; Rueda-Romero et al., 2012; Yamaguchi et al., 2010; Rademacher et al., 2011) (Yadegari et al., 2000; Wang et al., 2006). Transcription factor-inducible lines were obtained from the TRANSPLANTA collection (Coego et al., 2014).

Plants were grown under standard conditions at 24°C in a 16-h light 8-h dark cycle. For root analyses, plants surfaced sterilized and sown in 1% Sucrose Murashige and Skoog (1% MS) medium. Seeds were stratified for 3 days at 4°C and dark and then transferred and kept vertical into a Percival growth chamber with a light intensity of $\sim 700 \text{ mol} \cdot \text{m}^{-2} \text{ s}^{-1}$ illuminated by a daylight-white fluorescence lamp (FL40SS ENW/37; PANASONIC). Selection of transgenic seedlings were performed in 1% MS medium supplemented with 50 mg L⁻¹ kanamycin or 15 mg L⁻¹ Glufosinate ammonium, depending on the transgene.

Cloning strategies

All oligonucleotides used in this study are described in Supplemental Data Set 4. All PCR-amplified fragments were completely sequenced after subcloning, and only the clones without PCR-induced errors were used for subsequent cloning steps. For promoter amplification, Col-0 genomic DNA was used as template. For coding region amplification, Col-0 cDNA was used as template, except for the *CLF* coding region, which was amplified from genomic DNA and thus contains introns. For the generation of the transcriptional GUS fusions, each respective PCR product was introduced into pENTR D-TOPO (Invitrogen) and subsequently recombined into the pGWB4 and pGWB5 destination vectors (Nakagawa et al., 2007) with the exception of the *CLF* promoter, which was assembled to Venus-N7 (rapidly folding YFP variant) by Hot Fusion reaction (Fu et al., 2014) into the Bsal digested pGoldenGate-Se7 (Shahram Emami, 2013).

For the CLF translational fusion shown in Figure 2, the *CLF* genomic region was amplified (primers CLF_TOPO_F_NO_ATG/CLF_R) and introduced into pENTR™/D-Topo® (Invitrogen). The gCLF_D_Topo clone was introduced into the pB7WGC2 binary vector to generate a CFP:gCLF fusion. The ECFP:gCLF sequence was then amplified (ECFP_TOPO_F/CLF_R) and introduced into pENTR™/D-Topo®. The -2842 DNA

sequence corresponding to the *CLF* promoter was amplified (pCLF_F/pCLF_R) and cloned into pENTR 5'TA-TOPO®. A MultiSite Gateway reaction was performed using CLFpro-TA-Topo, CFP:gCLF-D-Topo and the pK7m34GW destination vector. The CLFpro:CFP:gCLF transgene was introduced into the *clf-29* background by floral dip transformation {Clough:1998uf}, and a complementation assay was performed on T2 plants to validate a 3:1 segregation ratio. For the *CLF* genomic fusion shown in Supplemental Figure 7B, a genomic region of *CLF* including 2175 bp upstream from the start codon and 1010 bp downstream from the stop codon was amplified with primers D-TOPO-genomic_CLF_s2 and genomic_CLF_as2, following with primers genomic_CLF_s1 and genomic_CLF_as1, using PrimeSTAR® Max DNA polymerase (Takara). The PCR product was cloned into pENTR™/D-Topo® (Thermo Fisher scientific), and an error-free entry clone, pENTR-gCLF, was confirmed by sequence analyses. A mGFP sequence with a GGS-linker at its N-terminus was inserted into pENTR-gCLF at the site before the stop codon of CLF in frame by CPEC (circular polymerase extension cloning) method, following the amplification of pENTR-gCLF and linker-mGFP with primers CLF ter_s and CLF body-Δstop_as and primers CLF body-mGFP_s and mGFP-CLF ter_as, respectively. A recombination reaction was performed between the resulting entry clone, pENTR-gCLF-mGFP, and destination vector pGWB501 (Nakagawa et al., 2007) using LR Clonase II enzyme mix (Invitrogen™). Error-free destination clone was confirmed by sequence analyses and introduced into *Agrobacterium tumefaciens* strain GV3101::pMP90 by electroporation. The transgene was introduced into the *clf-28+/-; swm-7/-* background by floral dip transformation of *clf-28+/-; swm-7/-* plants. A complementation assay was performed to validate the function of the fusion protein. For the other translational GFP fusions, gene promoters were also introduced into pENTR 5'TA-TOPO®; gene cDNAs were introduced into pENTR D-TOPO, and the *mGFP5* reporter gene was introduced into pDONOR P2r-P3. Plasmids containing the promoter, gene and *GFP* were introduced into pB7m34GW (Karimi et al., 2005) by a Multisite Gateway reaction (Invitrogen).

The design of the artificial miRNA for *MSI1* was performed following WMD3 software (Ossowski et al., 2008) and cloned into pENTR D-TOPO. Afterwards, a Multisite Gateway reaction was performed in combination with the promoter of *WOODEN LEG* (kindly provided by Anthony Bishopp -University of Nottingham) and pK7m24GW (Karimi et al., 2005). The resulting plasmids were introduced into *Agrobacterium tumefaciens* strain GV3101 carrying the pSoup plasmid (Hellens et al., 2000), and Col-0 wild type in addition

to MSI1_{pro}:MSI1:GFP were transformed using floral dip (Clough and Bent, 1998). Transformation into the MSI1_{pro}:MSI1:GFP background served as a control to ensure precise tissue-specific silencing of MSI1 with the designed artificial miRNA.

Arabidopsis cross-sections

Five-day-old roots were embedded in 3% agarose (PELCO® 21 Cavity EM Embedding Mold) and incubated overnight at 4°C in Fixation Buffer (2.5% glutaldehyde + 2% paraformaldehyde in phosphate buffer 0.2M (pH 7). Dehydration was performed by incubating the sample for 2h in serial dilutions of ethanol (20%, 40%, 60%, 80%, 90% and 95%). The sample was plastic embedded by performing the following steps: 2 hours incubation in 1:1 Ethanol:Acetone, 2 hours incubation in 100% Acetone, 12 hours incubation in 7:1 Acetone:Spurr's resin, 12 hours incubation in 3:1 Acetone:Spurr's resin, 12 hours incubation in 100% Spurr's resin, 12 hours incubation in Spurr's resin. The resin was polymerized at 70°C for 12 hours. Blocks were trimmed and 1.5 µm cross-sections were produced with a Leica 2050 SuperCut microtome. Toluidine blue staining (0.1% of Toluidine blue in 0.1M Phosphate buffer pH 6.8) was performed before microscopic analysis.

The mPS-PI staining method (Truernit et al., 2008) combined with confocal microscopy was used for the acquisition of high resolution root longitudinal and Z-stack images of ARF17ox plants under Mock and β-Estradiol treatments.

Gene regulatory network mapping

Promoter sequences for PRC2 genes are described in Supplemental Data Set 2. Yeast One Hybrid Screening was performed as described (Gaudinier et al., 2011). Correlations between predicted transcription factors and targets were determined using root spatial temporal microarray datasets found in Brady et al. 2007. For simplicity, the data were transformed to contain the Log(2) mean expression value for each sample. A Pearson correlation was calculated for each network-predicted TF-promoter interaction set. Interactions with a Benjamini-Hochberg FDR corrected p-value less than or equal to 0.05 were considered significant. P-values for the Benjamini-Hochberg correction were determined from correlations of all possible TF-promoter combinations of each node within the network.

Validation and the direction of the yeast one hybrid interactions were characterized *in vivo* by performing *trans*-activation assays in *Nicotiana benthamiana* leaves and gene expression analyses in Arabidopsis estradiol-inducible transcription factor lines. For *trans*-activation assays transcription factors in PYL436 (effector) (Ma et al., 2013), collection kindly provided by Dinesh Kumar – UC Davis, promoter:GUS (reporter), 35S_{pro}:LUCIFERASE (internal control) and p19 (RNA silencing inhibitor) constructs were transformed into Agrobacterium tumefaciens (strain GV3101) and used as described in (Taylor-Teeple et al., 2015). In Arabidopsis, 12 hour and 24 hour treatments in liquid 1% MS supplemented with 10 μ M β -Estradiol (from a 10mM stock in 100% DMSO) was used to induce the expression of each transcription factor in 5-day-old seedlings. Quantification of transcription factor and PRC2 gene expression was performed by Reverse-transcription-quantitative PCR. We calculated the mean from 3 independent experiments (biological replicates) and from the average of 3 technical replicates per biological replicate. Each biological replicate captures expression from approximately 200 roots of each respective genotype. In each case, the $\Delta\Delta$ Ct was calculated relative to a Ubiquitin10 control (At4g05320). In all cases, significance was tested using a t-test. * = p<.05; ** = p<.01; *** = p<.001.

We used Cytoscape software (Shannon et al., 2003) for data visualization and GO analysis of the network.

Whole mount H3K27me3 immunohybridization of Arabidopsis roots

The protocol was adapted from (She et al., 2014). Roots of 5-day-old plants were fixed in fixation buffer (1xPBS, 2mM EGTA, 1% Formaldehyde, 10% DMSO and 1% Tween-20) for 30 minutes at room temperature and then mounted in 5% Acrylamide on a microscope slide. Samples were fixed by incubating them for 5 minutes in 100% ethanol, 5 minutes in 100% methanol, 30 minutes in methanol:xylene (1:1), 5 minutes in methanol, 5 minutes in ethanol and 15 minutes in methanol:PBS (1.37M NaCl, 27mM KCl, 100mM Na₂HPO₄, 18mM KH₂PO₄, pH 7.4) + 0.1% Tween 20 (1:1) + 2.5% Formaldehyde. The samples were then rinsed with PBS + 0.1% Tween 20 and cell walls were digested for 2h at 37°C with cell wall digestion solution (0.5% cellulase, 1% driselase, 0.5% pectolyase in PBS). After rinsing with PBS + 0.1% Tween 20, the samples were permeabilized in PBS + 2% Tween 20 for 2 hours. Immunodetection was performed using antibodies against H3K27me3 (Millipore 07-449), H3K4me3 (Millipore 07-473) and H3 (ab1791) as a control at 0.01 μ g/ μ l final concentration each, for 14 hours. Samples were washed for 4hours with PBS + 0.1%

Tween 20 and incubated for 12h with goat anti-rabbit (alexa fluor 488 conjugate) secondary antibody (Life Technologies A-11034A). Samples were washed with 1x PBS + 0.1% Tween-20 for 1 hour and nuclei were counterstained with propidium iodide at a concentration of 5 µg/ml for 15 min, rinsed with PBS + 0.1% Tween 20, and mounted in Prolong Gold (Invitrogen) + 5 µg/ml propidium iodide. Samples were imaged using a Zeiss 700 (Genome Center – University of California, Davis). Simultaneous detection of Alexa fluor 488 and Propidium iodide signal was performed using the same settings among the different samples/mutants (10-15 roots were studied for each mutant line).

Fluorescence Activated Cell Sorting

Arabidopsis WOL_{pro}:GFP root protoplast were prepared as described in (Brady et al., 2007). The MoFlo cell sorter's electronic configuration was modified to identify intact protoplasts above electronic and sample buffer "noise" levels by choosing a side scatter electronic threshold and by applying logarithmic scaling to the forward angle and side angle 488nm laser light scatter signals. To collect the GFP-positive protoplasts, the green fluorescence of the GFP (530/50 detection filter) was separated from the red fluorescence (emission 670/30) of chlorophyll (Supplemental Figure 5). Protoplast chromatin was crosslinked with 0.1% formaldehyde for 5 min and the reaction was stopped by adding glycine (0.125M final concentration).

Chromatin Immunoprecipitation assay

The chromatin immunoprecipitation assay performed in this study is a modification of the protocol described in (Bouyer et al., 2011). We used four independent biological replicates (100,000 GFP positive protoplast each) and two antibodies: H3K27me3 (Millipore 07-449) and H3K4me3 (Millipore 07-473). DNA recovered after ChIP and the input chromatin were both amplified using a SeqPlex Enhanced DNA amplification kit (SEQXE – Sigma) following the manufacturer's instructions. Amplified DNA was used to synthesize a barcoded Illumina-compatible library (Kumar et al., 2012). Libraries were pooled and sequenced on the HiSeq2000 in the 50SR mode.

ChIPseq data analysis

Reads were filtered by length and quality and aligned to the Arabidopsis (TAIR10) genome using Bowtie (Langmead et al., 2009) and the parameters "-v2 -m1 --best --strata -S". SCICER software was used to determine the differentially methylated islands using a 200bp window size, 200bp gap size and an FDR of 0.005. The genomic regions containing the histone modification was determined using windowbed software (Quinlan and Hall,

2010) and -1000bp upstream and downstream of the gene body for H3K27me3 and 200bp upstream and 200bp downstream for H3K4me3. Genes that overlap in at least 3 of the 4 biological replicates were considered as high confidence genes for the downstream analyses.

Root cell type-specific expression of the H3K27me3 and H3K4me3 affected genes was obtained from (Brady et al., 2007). Raw expression values were log₂ transformed and graphed with R software and the ggplot2 package.

GUS expression analysis in Arabidopsis

Plant tissue was fixed in 90% acetone for 30 minutes and washed twice with water before GUS staining. Roots were submerged in the GUS staining solution (50mM Phosphate buffer, 0.2% Triton TX-100, 1.5mM Potassium Ferrocyanide, 1.5mM Potassium Ferricyanide and 2mM X-Gluc (5-bromo-4-chloro-3-indolyl β -D-glucuronide cyclohexamine salt dissolved in DMSO – Gold Biotechnology G1281C1), infiltrated under vacuum for 5 minutes, and incubated at 37°C in the dark for 18 hours. Roots were then washed with increasing concentrations of diluted ethanol (20%, 35%, 50% and 70%) and then mounted with Hoyer's solution on microscope slides. The activity of the GUS reporter gene was observed under a Zeiss Axioscope 2 Fluorescence microscope.

***In situ* hybridization**

The ARF17 and CLF coding region was PCR amplified using Col0 cDNA and the set of primers "ARF17_cDNA_F"/"ARF17_cDNA_R" and "CLF_TOPO_F_NO_ATG"/"CLF_R(no_STOP)". PCR product was cloned into pGEMTeasy (PROMEGA). Fluorescein labeled sense and antisense probes were performed as manufacturer indications (Fluorescein RNA Labeling Mix - Roche). Tissue fixation, permeabilization, probe hybridization and detection were adapted from (Bruno et al., 2011). Probe detection was performed using HRP conjugated anti-FITC antibody (1:100 dilution) (AB6656, Abcam), followed by tyramide signal amplification (TSA™ Reagent, Alexa Fluor® 488 Tyramide – Molecular probes (T20948)). Tissue was then counter stained with propidium iodide (5ug/mL) for 5 min, rinsed in water, and the samples were mounted with antifade reagent (Prolong gold – Molecular probes –(P36941)). Samples were imaged using a Zeiss 880 with Ayriscan (SBBS –Durham University). Simultaneous detection of Alexa fluor 488 and Propidium Iodide signal was performed using the same settings among the different samples (10-15 roots were studied for each mutant line).

615

616 **Accession numbers**

617 Sequence data from this article can be found in the GenBank/EMBL libraries under
618 accession numbers GSE86429. Accession numbers of major genes mentioned are as
619 follows: CLF = At2g23380; SWN = At4g02020; DOF6 = At3g45610; VND7 = At1g71930;
620 FIE = At3g20740; ARF17 = At1g77850; MEA = At1g02580; MSI1 = At5g58230; FIS2 =
621 At2g35670; EMF2 = At5g51230; VRN2 = At4g16845.

622

623 **Supplemental Data**

624 **Supplemental Figure 1.**

625 Transcriptional profile of PRC2 genes in the Arabidopsis root.

626 **Supplemental Figure 2.** DOF6 OX root phenotype, DOF6 and CLF root expression and
627 CLF protein abundance in the *clf28swn7* background.

628 **Supplemental Figure 3.** ARF17ox ectopic cell proliferation data, CLFpro:CFP:CLF
629 complementation assay and ARF17 RNA in-situ sense control.

630 **Supplemental Figure 4.** Whole-mount immunostaining of H3K27me3 and H3K4me3
631 deposition in Arabidopsis PRC2 mutant roots.

632 **Supplemental Figure 5.** Root cellular resolution phenotypes of different PRC2 mutants

633 **Supplemental Figure 6.** Whole-mount immunostaining of H3K27me3 in the
634 pWOL:amiRNA_MSI1 Arabidopsis line.

635 **Supplemental Figure 7.** Vascular-specific analysis of H3K27me3 deposition for the
636 fluorescence activated cell sorting of the stele (WOLpro:GFP).

637 **Supplemental Figure 8.** Transcriptional profiles of the transcription factors upstream of
638 PRC2 genes.

639 **Supplemental Data Set 1:** H3K27me3 and H3K4me3 genes in the vascular cylinder and
640 whole root and associated GO categories.

641 **Supplemental Data Set 2:** Protein-DNA Interaction Network and promoter sequences for
642 the different PRC2 genes studied.

643 **Supplemental Data Set 3:** PRC2 Network Validation.

644 **Supplemental Data Set 4:** Primer sequences.

645

ACKNOWLEDGMENTS

MDL was supported by an EMBO and HFSP postdoctoral fellowships. SMB and FR were supported by the France-Berkeley Fund. SMB was supported by a Katherine Esau Junior Faculty Fellowship and a Hellman Fellowship. Work in the Colot's lab was supported by the European Union Seventh Framework Programme Network of Excellence EpiGeneSys and the CNRS (AKM, EC and FR). AKM is the recipient of a grant from the French Ministère de la Recherche et de l'Enseignement Supérieur. Work in the Sugimoto lab was supported by the Grant-in-Aid for Scientific Research on Priority Areas to KS (26291064). This project was supported by the University of California Davis Flow Cytometry Shared Resource Laboratory with funding from the NCI P30 CA0933730, and NIH NCRR C06-RR12088, S10 RR12964 and S10 RR 026825 grants and with technical assistance from Ms. Bridget McLaughlin and Mr. Jonathan Van Dyke. We would like to thank Judy Jernstedt for providing us access to a microtome and to Niko Geldner and Peter Etchells for critical reading of the manuscript.

AUTHOR CONTRIBUTIONS

M.D.L. designed and performed experiments, analyzed data, discussed results, and wrote the article. L.P. performed experiments and analyzed data. G.T performed computational analyses. A.G. performed experiments. A.K.M., H.H, D.K, and M.R performed experiments. K.S designed experiments with H.H and analyzed data. F.R. designed experiments with A.K.M, and contributed to writing the manuscript. S.M.B. designed experiments, discussed results, and wrote the article

REFERENCES

- Aichinger, E., Villar, C.B.R., Di Mambro, R., Sabatini, S., and Kohler, C.** (2011). The CHD3 Chromatin Remodeler PICKLE and Polycomb Group Proteins Antagonistically Regulate Meristem Activity in the Arabidopsis Root. *The Plant Cell* **23**: 1047–1060.
- Aichinger, E., Villar, C.B.R., Farrona, S., Reyes, J.C., Hennig, L., and Köhler, C.** (2009). CHD3 Proteins and Polycomb Group Proteins Antagonistically Determine Cell Identity in Arabidopsis. *PLoS Genet* **5**: e1000605.
- Aldiri, I. and Vetter, M.L.** (2009). Characterization of the expression pattern of the PRC2 core subunit Suz12 during embryonic development of *Xenopus laevis*. *Dev. Dyn.* **238**: 3185–3192.
- Bemer, M. and Grossniklaus, U.** (2012). Dynamic regulation of Polycomb group activity

during plant development. *Curr. Opin. Plant Biol.* **15**: 523–529.

Benfey, P.N. and scheres, B. (2000). Root development. *Curr. Biol.* **10**: R813–5.

Birnbaum, K., Shasha, D.E., Wang, J.Y., and Jung, J.W. (2003). A gene expression map of the Arabidopsis root. *Science*.

Bouyer, D., Roudier, F., Heese, M., Andersen, E.D., Gey, D., Nowack, M.K., Goodrich, J., Renou, J.-P., Grini, P.E., Colot, V., and Schnittger, A. (2011). Polycomb Repressive Complex 2 Controls the Embryo-to-Seedling Phase Transition. *PLoS Genet* **7**: e1002014.

Bracken, A.P., Pasini, D., Capra, M., Prosperini, E., Colli, E., and Helin, K. (2003). EZH2 is downstream of the pRB-E2F pathway, essential for proliferation and amplified in cancer. *The EMBO Journal* **22**: 5323–5335.

Brady, S.M. et al. (2011). A stele-enriched gene regulatory network in the Arabidopsis root. *Molecular Systems Biology* **7**: 459.

Brady, S.M., Orlando, D.A., Lee, J.Y., Wang, J.Y., Koch, J., Dinneny, J.R., Mace, D., Ohler, U., and Benfey, P.N. (2007). A High-Resolution Root Spatiotemporal Map Reveals Dominant Expression Patterns. *Science* **318**: 801–806.

Bruno, L., Muto, A., Spadafora, N.D., Iaria, D., Chiappetta, A., Van Lijsebettens, M., and Bitonti, M.B. (2011). Multi-probe in situ hybridization to whole mount Arabidopsis seedlings. *Int. J. Dev. Biol.* **55**: 197–203.

Chanvivattana, Y., Bishopp, A., Schubert, D., Stock, C., Moon, Y.-H., Sung, Z.R., and Goodrich, J. (2004). Interaction of Polycomb-group proteins controlling flowering in Arabidopsis. *Development* **131**: 5263–5276.

Ciferri, C., Lander, G.C., Maiolica, A., Herzog, F., Aebersold, R., and Nogales, E. (2012). Molecular architecture of human polycomb repressive complex 2. *Elife* **1**: e00005.

Clough, S.J. and Bent, A.F. (1998). Floral dip: a simplified method for *Agrobacterium*-mediated transformation of *Arabidopsis thaliana*. *The Plant Journal*.

Coego, A., Brizuela, E., Castillejo, P., Ruíz, S., Koncz, C., Del Pozo, J.C., Pineiro, M., Jarillo, J.A., Paz-Ares, J., León, J., The TRANSPLANTA Consortium (2014). The TRANSPLANTA collection of Arabidopsis lines: a resource for functional analysis of transcription factors based on their conditional overexpression. *The Plant Journal*.

De Lucia, F., Crevillen, P., Jones, A.M.E., Greb, T., and Dean, C. (2008). A PHD-polycomb repressive complex 2 triggers the epigenetic silencing of FLC during vernalization. *Proceedings of the National Academy of Sciences* **105**: 16831–16836.

De Rybel, B. et al. (2014). Integration of growth and patterning during vascular tissue formation in Arabidopsis. *Science* **345**: 1255215–1255215.

Deal, R.B. and Henikoff, S. (2010). A Simple Method for Gene Expression and Chromatin Profiling of Individual Cell Types within a Tissue. *Developmental Cell* **18**: 1030–1040.

718 **Deng, W., Buzas, D.M., Ying, H., Robertson, M., Taylor, J., Peacock, W.J., Dennis,**
719 **E.S., and Helliwell, C.** (2013). Arabidopsis Polycomb Repressive Complex 2 binding
720 sites contain putative GAGA factor binding motifs within coding regions of genes. *BMC*
721 *Genomics* **14**: 593.

722 **Derkacheva, M., Steinbach, Y., Wildhaber, T., Mozgová, I., Mahrez, W., Nanni, P.,**
723 **Bischof, S., Gruissem, W., and Hennig, L.** (2013). Arabidopsis MSI1 connects LHP1
724 to PRC2 complexes. *The EMBO Journal*.

725 **Dolan, L., Janmaat, K., Willemsen, V., Linstead, P., Poethig, S., Roberts, K., and**
726 **scheres, B.** (1993). Cellular organisation of the *Arabidopsis thaliana* root.
727 *Development* **119**: 71–84.

728 **Du, Z., Zhou, X., Ling, Y., Zhang, Z., and Su, Z.** (2010). agriGO: a GO analysis toolkit for
729 the agricultural community. *Nucleic Acids Res.* **38**: W64–70.

730 **Etchells, J.P. and Turner, S.R.** (2010). Orientation of vascular cell divisions in
731 *Arabidopsis*. *Plant Signal Behav* **5**: 730–732.

732 **Etchells, J.P., Provost, C.M., Mishra, L., and Turner, S.R.** (2013). WOX4 and WOX14
733 act downstream of the PXY receptor kinase to regulate plant vascular proliferation
734 independently of any role in vascular organisation. *Development* **140**: 2224–2234.

735 **Fasano, C.A., Dimos, J.T., Ivanova, N.B., Lowry, N., Lemischka, I.R., and Temple, S.**
736 (2007). shRNA knockdown of Bmi-1 reveals a critical role for p21-Rb pathway in NSC
737 self-renewal during development. *Cell Stem Cell* **1**: 87–99.

738 **Fisher, K. and Turner, S.** (2007). PXY, a receptor-like kinase essential for maintaining
739 polarity during plant vascular-tissue development. *Curr. Biol.* **17**: 1061–1066.

740 **Fu, C., Donovan, W.P., Shikapwashya-Hasser, O., Ye, X., and Cole, R.H.** (2014). Hot
741 Fusion: An Efficient Method to Clone Multiple DNA Fragments as Well as Inverted
742 Repeats without Ligase. *PLoS ONE* **9**: e115318.

743 **Gaudinier, A. et al.** (2011). Enhanced Y1H assays for *Arabidopsis*. *Nat Meth* **8**: 1053–
744 1055.

745 **Gu, X., Xu, T., and He, Y.** (2014). A histone H3 lysine-27 methyltransferase complex
746 represses lateral root formation in *Arabidopsis thaliana*. *Molecular Plant* **7**: 977–988.

747 **He, C., Chen, X., Huang, H., and Xu, L.** (2012). Reprogramming of H3K27me3 Is Critical
748 for Acquisition of Pluripotency from Cultured *Arabidopsis* Tissues. *PLoS Genet* **8**:
749 e1002911.

750 **Helin, K. and Dhanak, D.** (2013). Chromatin proteins and modifications as drug targets.
751 *Nature* **502**: 480–488.

752 **Hellens, R.P., Edwards, E.A., Leyland, N.R., Bean, S., and Mullineaux, P.M.** (2000).
753 pGreen: a versatile and flexible binary Ti vector for *Agrobacterium*-mediated plant
754 transformation. *Plant Mol Biol* **42**: 819–832.

755 **Hennig, L. and Derkacheva, M.** (2009). Diversity of Polycomb group complexes in plants:
756 same rules, different players? *Trends in Genetics* **25**: 414–423.

757 **Hennig, L., Taranto, P., Walser, M., Schönrock, N., and Grissem, W.** (2003).
758 *Arabidopsis* MSI1 is required for epigenetic maintenance of reproductive development.
759 *Development* **130**: 2555–2565.

760 **Hirabayashi, Y., Suzuki, N., Tsuboi, M., Endo, T.A., Toyoda, T., Shinga, J., Koseki, H.,**
761 **Vidal, M., and Gotoh, Y.** (2009). Polycomb limits the neurogenic competence of
762 neural precursor cells to promote astrogenic fate transition. *Neuron* **63**: 600–613.

763 **Ikeuchi, M. et al.** (2015). PRC2 represses dedifferentiation of mature somatic cells in
764 *Arabidopsis*. *Nature Plants* **1**: 15089.

765 **Inoue, T., Higuchi, M., Hashimoto, Y., Seki, M., Kobayashi, M., Kato, T., Tabata, S.,**
766 **Shinozaki, K., and Kakimoto, T.** (2001). Identification of CRE1 as a cytokinin
767 receptor from *Arabidopsis*. *Nature* **409**: 1060–1063.

768 **Jullien, P.E., Mosquna, A., Ingouff, M., Sakata, T., Ohad, N., and Berger, F.** (2008).
769 Retinoblastoma and its binding partner MSI1 control imprinting in *Arabidopsis*. *Plos*
770 *Biol* **6**: e194.

771 **Karimi, M., De Meyer, B., and Hilson, P.** (2005). Modular cloning in plant cells. *Trends in*
772 *Plant Science*.

773 **Kinoshita, T., Harada, J.J., Goldberg, R.B., and Fischer, R.L.** (2001). Polycomb
774 repression of flowering during early plant development. *Proc. Natl. Acad. Sci. U.S.A.*
775 **98**: 14156–14161.

776 **Kleer, C.G. et al.** (2003). EZH2 is a marker of aggressive breast cancer and promotes
777 neoplastic transformation of breast epithelial cells. *Proc. Natl. Acad. Sci. U.S.A.* **100**:
778 11606–11611.

779 **Köhler, C., Hennig, L., Bouveret, R., Gheyselinck, J., Grossniklaus, U., and Grissem,**
780 **W.** (2003). *Arabidopsis* MSI1 is a component of the MEA/FIE Polycomb group complex
781 and required for seed development. *The EMBO Journal* **22**: 4804–4814.

782 **Köhler, C., Page, D.R., Gagliardini, V., and Grossniklaus, U.** (2005). The *Arabidopsis*
783 *thaliana* MEDEA Polycomb group protein controls expression of PHERES1 by parental
784 imprinting. *Nat Genet* **37**: 28–30.

785 **Kubo, M.** (2005). Transcription switches for protoxylem and metaxylem vessel formation.
786 *Genes & Development* **19**: 1855–1860.

787 **Kumar, R., Ichihashi, Y., Kimura, S., Chitwood, D.H., Headland, L.R., Peng, J., Maloof,**
788 **J.N., and Sinha, N.R.** (2012). A high-throughput method for Illumina RNA-Seq library
789 preparation. *Front Plant Sci* **3**.

790 **Kuzmichev, A., Margueron, R., Vaquero, A., Preissner, T.S., Scher, M., Kirmizis, A.,**
791 **Ouyang, X., Brockdorff, N., Abate-Shen, C., Farnham, P., and Reinberg, D.** (2005).
792 Composition and histone substrates of polycomb repressive group complexes change
793 during cellular differentiation. *Proc. Natl. Acad. Sci. U.S.A.* **102**: 1859–1864.

794 **Lafos, M., Kroll, P., Hohenstatt, M.L., Thorpe, F.L., Clarenz, O., and Schubert, D.**
795 (2011). Dynamic regulation of H3K27 trimethylation during *Arabidopsis* differentiation.
796 *PLoS Genet* **7**: e1002040.

797 **Langmead, B., Trapnell, C., Pop, M., and Salzberg, S.L.** (2009). Ultrafast and memory-
798 efficient alignment of short DNA sequences to the human genome. *Genome Biol* **10**:
799 R25.

800 **Laugesen, A. and Helin, K.** (2014). Chromatin repressive complexes in stem cells,
801 development, and cancer. *Cell Stem Cell* **14**: 735–751.

802 **Lee, J.-Y., Colinas, J., Wang, J.Y., Mace, D., Ohler, U., and Benfey, P.N.** (2006).
803 Transcriptional and posttranscriptional regulation of transcription factor expression in
804 *Arabidopsis* roots. *Proc. Natl. Acad. Sci. U.S.A.* **103**: 6055–6060.

805 **Ma, S., Shah, S., Bohnert, H.J., Snyder, M., and Dinesh-Kumar, S.P.** (2013).
806 Incorporating motif analysis into gene co-expression networks reveals novel modular
807 expression pattern and new signaling pathways. *PLoS Genet* **9**: e1003840.

808 **Mahonen, A.P.** (2000). A novel two-component hybrid molecule regulates vascular
809 morphogenesis of the *Arabidopsis* root. *Genes & Development* **14**: 2938–2943.

810 **Mahonen, A.P.** (2006). Cytokinin Signaling and Its Inhibitor AHP6 Regulate Cell Fate
811 During Vascular Development. *Science* **311**: 94–98.

812 **Mallory, A.C.** (2005). MicroRNA-Directed Regulation of *Arabidopsis* AUXIN RESPONSE
813 FACTOR17 Is Essential for Proper Development and Modulates Expression of Early
814 Auxin Response Genes. *THE PLANT CELL ONLINE* **17**: 1360–1375.

815 **Margueron, R. and Reinberg, D.** (2011). The Polycomb complex PRC2 and its mark in
816 life. *Nature* **469**: 343–349.

817 **Margueron, R., Li, G., Sarma, K., Blais, A., Zavadil, J., Woodcock, C.L., Dynlacht,
818 B.D., and Reinberg, D.** (2008). Ezh1 and Ezh2 maintain repressive chromatin through
819 different mechanisms. *Molecular Cell* **32**: 503–518.

820 **Mozgová, I. and Hennig, L.** (2015). The Polycomb Group Protein Regulatory Network.
821 <http://dx.doi.org/10.1146/annurev-arplant-043014-115627>.

822 **Nakagawa, T., Kurose, T., Hino, T., Tanaka, K., Kawamukai, M., Niwa, Y., Toyooka, K.,
823 Matsuoka, K., Jinbo, T., and Kimura, T.** (2007). Development of series of gateway
824 binary vectors, pGWBs, for realizing efficient construction of fusion genes for plant
825 transformation. *J. Biosci. Bioeng.* **104**: 34–41.

826 **Ohno, K., McCabe, D., Czermin, B., Imhof, A., and Pirrotta, V.** (2008). ESC, ESCL and
827 their roles in Polycomb Group mechanisms. *Mech. Dev.* **125**: 527–541.

828 **Okushima, Y.** (2005). Functional Genomic Analysis of the AUXIN RESPONSE FACTOR
829 Gene Family Members in *Arabidopsis thaliana*: Unique and Overlapping Functions of
830 ARF7 and ARF19. *The Plant Cell* **17**: 444–463.

831 **Ossowski, S., Schwab, R., and Weigel, D.** (2008). Gene silencing in plants using artificial
832 microRNAs and other small RNAs. *The Plant Journal* **53**: 674–690.

833 **Pasini, D., Bracken, A.P., Hansen, J.B., Capillo, M., and Helin, K.** (2007). The
834 polycomb group protein Suz12 is required for embryonic stem cell differentiation. *Mol.*
835 *Cell. Biol.* **27**: 3769–3779.

836 **Quinlan, A.R. and Hall, I.M.** (2010). BEDTools: a flexible suite of utilities for comparing
837 genomic features. *Bioinformatics* **26**: 841–842.

838 **Rademacher, E.H., Möller, B., Lokerse, A.S., Llavata-Peris, C.I., van den Berg, W.,**
839 **and Weijers, D.** (2011). A cellular expression map of the Arabidopsis AUXIN
840 RESPONSE FACTOR gene family. *The Plant Journal* **68**: 597–606.

841 **Reece-Hoyes, J.S. et al.** (2011). Yeast one-hybrid assays for gene-centered human gene
842 regulatory network mapping. *Nat Meth* **8**: 1050–1052.

843 **Roudier, F. et al.** (2011). Integrative epigenomic mapping defines four main chromatin
844 states in Arabidopsis. *The EMBO Journal* **30**: 1928–1938.

845 **Rueda-Romero, P., Barrero-Sicilia, C., Gómez-Cadenas, A., Carbonero, P., and**
846 **Oñate-Sánchez, L.** (2012). Arabidopsis thaliana DOF6 negatively affects germination
847 in non-after-ripened seeds and interacts with TCP14. *Journal of Experimental Botany*
848 **63**: 1937–1949.

849 **Scheres, B.** (2007). Stem-cell niches: nursery rhymes across kingdoms. *Nature Reviews*
850 *Molecular Cell Biology* **8**: 345–354.

851 **Shahram Emami, M.-C.Y.J.R.D.** (2013). A robust family of Golden Gate Agrobacterium
852 vectors for plant synthetic biology. *Front Plant Sci* **4**.

853 **Shannon, P., Markiel, A., Ozier, O., Baliga, N.S., Wang, J.T., Ramage, D., Amin, N.,**
854 **Schwikowski, B., and Ideker, T.** (2003). Cytoscape: a software environment for
855 integrated models of biomolecular interaction networks. *Genome Research* **13**: 2498–
856 2504.

857 **She, W., Grimanelli, D., and Baroux, C.** (2014). An efficient method for quantitative,
858 single-cell analysis of chromatin modification and nuclear architecture in whole-mount
859 ovules in Arabidopsis. *J Vis Exp*: e51530.

860 **Sher, F., Rössler, R., Brouwer, N., Balasubramaniyan, V., Boddeke, E., and Copray, S.**
861 (2008). Differentiation of neural stem cells into oligodendrocytes: involvement of the
862 polycomb group protein Ezh2. *Stem Cells* **26**: 2875–2883.

863 **Sieburth, L.E. and Meyerowitz, E.M.** (1997). Molecular dissection of the AGAMOUS
864 control region shows that cis elements for spatial regulation are located intragenically.
865 *The Plant Cell* **9**: 355–365.

866 **Stojic, L. et al.** (2011). Chromatin regulated interchange between polycomb repressive
867 complex 2 (PRC2)-Ezh2 and PRC2-Ezh1 complexes controls myogenin activation in
868 skeletal muscle cells. *Epigenetics Chromatin* **4**: 16.

869 **Takawa, M. et al.** (2011). Validation of the histone methyltransferase EZH2 as a
870 therapeutic target for various types of human cancer and as a prognostic marker.
871 *Cancer Sci.* **102**: 1298–1305.

872 **Taylor-Teeples, M. et al.** (2015). An Arabidopsis gene regulatory network for secondary
873 cell wall synthesis. *Nature* **517**: 571–575.

874 **Terpstra, I. and Heidstra, R.** (2009). Stem cells: The root of all cells. *Seminars in Cell &*

Developmental Biology **20**: 1089–1096.

Truernit, E., Bauby, H., Dubreucq, B., Grandjean, O., Runions, J., Barthelemy, J., and Palauqui, J.C. (2008). High-Resolution Whole-Mount Imaging of Three-Dimensional Tissue Organization and Gene Expression Enables the Study of Phloem Development and Structure in Arabidopsis. *THE PLANT CELL ONLINE* **20**: 1494–1503.

Turck, F., Roudier, F., Farrona, S., Martin-Magniette, M.-L., Guillaume, E., Buisine, N., Gagnot, S., Martienssen, R.A., Coupland, G., and Colot, V. (2007). Arabidopsis TFL2/LHP1 specifically associates with genes marked by trimethylation of histone H3 lysine 27. *PLoS Genet* **3**: e86.

Varambally, S., Dhanasekaran, S.M., Zhou, M., Barrette, T.R., Kumar-Sinha, C., Sanda, M.G., Ghosh, D., Pienta, K.J., Sewalt, R.G.A.B., Otte, A.P., Rubin, M.A., and Chinnaiyan, A.M. (2002). The polycomb group protein EZH2 is involved in progression of prostate cancer. *Nature* **419**: 624–629.

Wagener, N., Macher-Goeppinger, S., Pritsch, M., Hüsing, J., Hoppe-Seyler, K., Schirmacher, P., Pfitzenmaier, J., Haferkamp, A., Hoppe-Seyler, F., and Hohenfellner, M. (2010). Enhancer of zeste homolog 2 (EZH2) expression is an independent prognostic factor in renal cell carcinoma. *BMC Cancer* **10**: 524.

Wang, D., Tyson, M.D., Jackson, S.S., and Yadegari, R. (2006). Partially redundant functions of two SET-domain polycomb-group proteins in controlling initiation of seed development in Arabidopsis. *Proc. Natl. Acad. Sci. U.S.A.* **103**: 13244–13249.

Yadegari, R., Kinoshita, T., Lotan, O., Cohen, G., Katz, A., Choi, Y., Katz, A., Nakashima, K., Harada, J.J., Goldberg, R.B., Fischer, R.L., and Ohad, N. (2000). Mutations in the FIE and MEA genes that encode interacting polycomb proteins cause parent-of-origin effects on seed development by distinct mechanisms. *The Plant Cell* **12**: 2367–2382.

Yamaguchi, M., Ohtani, M., Mitsuda, N., Kubo, M., Ohme-Takagi, M., Fukuda, H., and Demura, T. (2010). VND-INTERACTING2, a NAC domain transcription factor, negatively regulates xylem vessel formation in Arabidopsis. *THE PLANT CELL ONLINE* **22**: 1249–1263.

Zhang, X., Clarenz, O., Cokus, S., Bernatavichute, Y.V., Pellegrini, M., Goodrich, J., and Jacobsen, S.E. (2007a). Whole-genome analysis of histone H3 lysine 27 trimethylation in Arabidopsis. *Plos Biol* **5**: e129.

Zhang, X., Germann, S., Blus, B.J., Khorasanizadeh, S., Gaudin, V., and Jacobsen, S.E. (2007b). The Arabidopsis LHP1 protein colocalizes with histone H3 Lys27 trimethylation. *Nat. Struct. Mol. Biol.* **14**: 869–871.

FIGURE LEGENDS

Figure 1. PRC2 genes are expressed in unique and overlapping cell types in the *Arabidopsis thaliana* root. For each genotype, the top panel shows the root meristem while the bottom panel shows the maturation/differentiation zone of the root. All images

were taken under the same acquisition conditions. **(A)** VRN2_{pro}:GUS expression. **(B)** EMF2_{pro}:GUS expression. **(C)** FIS2_{pro}:GUS expression. **(D)** SWN_{pro}:GUS expression. **(E)** CLF_{pro}:VenusN7 expression. **(F)** MEA_{pro}:GUS expression. **(G)** FIE_{pro}:GUS expression. **(H)** MSI1_{pro}:GUS expression. **(I)** Cartoon of the different cell types and tissues in the *Arabidopsis thaliana* root. **(J)** Promoter lengths of the different PRC2 genes used in the reporter lines. Translational start site = TSS.

Figure 2: PRC2 proteins are found in unique and overlapping cell types in the *Arabidopsis thaliana* root. For each genotype, the left panel shows the root meristem while the right panel shows the maturation/differentiation zone of the root. **(A)** VRN2_{pro}:VRN2:GUS **(B)** EMF2_{pro}:EMF2:GFP **(C)** SWN_{pro}:SWN:GFP **(D)** MEA_{pro}:MEA:YFP in *mea-3* **(E)** CLF_{pro}:CFP:gCLF in *clf-29*, **(F)** MSI1_{pro}:MSI1:GFP **(G)** FIE_{pro}:FIE:GFP in *fie-1*.

Figure 3: PRC2 regulates cell proliferation in the root meristem and vascular cylinder. **(A-B)** Whole mount immunostaining with antibodies specific for H3K27me3 (green in the wild-type Col-0) **(A)** and in the *clf-28 swn-7* double mutant **(B)**. Nuclear staining is indicated with white arrows. A magnified nucleus is shown in the inset. **(C-D)** Differential Interference Contrast image of the root meristem of the wild-type Col-0 **(C)** and the *clf-28 swn-7* double mutant **(D)**. White lines indicate the root meristematic zone (MZ). **(E-H)** Cross-sections showing the root vascular cylinder in wild-type Col-0 **(E)**, *clf-28 swn-7* **(F)**, *fie042* **(G)**, and in the WOL_{pro}:amiRNA_MSI line **(H)**. Green indicates pericycle cells, purple indicates procambium cells, red/orange indicates phloem cells. **(I-J)** The MSI protein is expressed ubiquitously throughout the *Arabidopsis thaliana* root **(I)** but is depleted specifically from the vascular cylinder in the WOL_{pro}:amiRNA_MSI1 line in the MSI1_{pro}:MSI1:GFP background (white arrows with one head) **(J)**. Note the reduction in the length of the root meristem (white arrow with two heads). **(K-L)** Differential interference contrast image showing two protoxylem pole cell files (black asterisk) in the wild-type Col-0 **(L)** and ectopic protoxylem (black asterisk) and metaxylem (blue asterisk) in the *fie042* mutant background **(L)**. **(M)** There are significantly more procambium and phloem and epidermal cells in the *clf-28 swn-7* mutant compared to wild-type Col-0. The reduction in *MSI1* expression shows increased number of cortical and endodermal cells but lower levels of cells in the stele. **(N)** The roots of *swn-7*, *clf-28 swn-7* and WOL_{pro}:amiRNA_MSI are significantly shorter than wild type Col-0 and *clf-29*. **(O)** There are more cells in the meristem of *clf-29* and fewer in *clf-28 swn-7* and WOL_{pro}:amiRNA_MSI relative to wild type (Col-0). In all cases, significance was tested using a t-test. * = p<.05; ** = p<.01; *** = p<.001. Error bars indicate the standard error value.

Figure 4. PRC2 regulates the balance between cell proliferation and differentiation in a tissue-specific manner in the *Arabidopsis thaliana* root. **(A)** Expression levels of genes marked by H3K27me3 in vascular cells relative to expression levels of genes marked by H3K4me3. Whole root and vascular-specific (pWOL:GFP positive) root protoplast were isolated by FACS and H3K27me3/H3K4me3 enriched regions were resolved by ChIPseq. Expression of the vascular specific H3K27me3 and H3K4me3 marked genes was determined using Brady et al. 2007 transcriptional data. **(B)** Number of genes marked by H3K27me3 in non-vascular cells. **(C-F)** Expression of a gene marked specifically by H3K27me3 and not expressed in vascular cells **(C,D)** ARF17_{pro}:GFP and of a gene marked specifically by H3K27me3 and not expressed in non-vascular cells VND7_{pro}:nYFP **(E,F)**. **(G-J)** Estradiol induction of the ARF17 transcription factor results in small regions of additional cell proliferation in the vascular cylinder **(I,J)** compared to the mock-treated root **(G,H)**. Asterisks indicate ectopic cell proliferation. **(K-L)** Estradiol induction of the VND7 transcription factor **(L)** results in ectopic xylem cell differentiation compared to a mock-treated root **(K)**.

Figure 5. Transcription factors regulating PRC2 gene expression *in planta*. Squares represent PRC2 gene promoters, circles represent transcription factors. A line between a transcription factor and promoter indicates that an interaction was observed by yeast one hybrid. A green line or a red line indicates that the transcription factor has been validated *in planta* as activating or repressing, respectively, the target gene *in planta* in either a trans-activation assay or upon B-estradiol induction of the transcription factor. Transcription factors are additionally colored according to their respective family. Transcription factors that interact with the most PRC2 gene promoters are indicated at the top of the network, while transcription factors that interact with just a single promoter are located just beside their respective PRC2 gene promoter. Network information is available in Supplemental Data Set 1.

Figure 6. Functional validation of a multi-tier PRC2 gene regulatory network (TF → PRC2 gene → H3K27me3 regulated gene). **(A)** β-estradiol induction (3 days) of the DOF6 transcription factor results in a significantly shorter root. Root inhibition caused by the induction of DOF6 is abolished in the *clf29* background. **(B)** ARF17 expression is activated in the *clf-29* mutant. **(C)** Induction of DOF6 results in a significant increase in the amount of CLF expression and a corresponding repression of ARF17 expression, as revealed by RT-qPCR. **(D)** Induction of DOF6 results in a significant increase in H3K27me3 deposition in the ARF17 loci in the root tissue. **(E)** DOF6 induction does not affect ARF17 expression

in the *clf-29* background. (F) Whole mount in-situ hybridization of *ARF17* mRNA. *ARF17* expression domain is expanded towards the vascular cylinder in the *clf-29* mutant. In all cases significance was tested using a t-test. * = $p < .05$; ** = $p < .01$; *** = $p < .001$. Error bars represent the standard error value of the \log_2 transformed expression. The mean is from 3 independent experiments (biological replicates), calculated from the average of 3 technical replicates per biological replicate. Each biological replicate captures expression from approximately 200 roots of each respective genotype. In each case, the $\Delta\Delta C_t$ was calculated relative to an ubiquitin10 control.

Parsed Citations

Aichinger, E., Villar, C.B.R., Di Mambro, R., Sabatini, S., and Kohler, C. (2011). The CHD3 Chromatin Remodeler PICKLE and Polycomb Group Proteins Antagonistically Regulate Meristem Activity in the Arabidopsis Root. *The Plant Cell* 23: 1047-1060.

Pubmed: [Author and Title](#)

CrossRef: [Author and Title](#)

Google Scholar: [Author Only](#) [Title Only](#) [Author and Title](#)

Aichinger, E., Villar, C.B.R., Farrona, S., Reyes, J.C., Hennig, L., and Köhler, C. (2009). CHD3 Proteins and Polycomb Group Proteins Antagonistically Determine Cell Identity in Arabidopsis. *PLoS Genet* 5: e1000605.

Pubmed: [Author and Title](#)

CrossRef: [Author and Title](#)

Google Scholar: [Author Only](#) [Title Only](#) [Author and Title](#)

Aldiri, I. and Vetter, M.L. (2009). Characterization of the expression pattern of the PRC2 core subunit Suz12 during embryonic development of *Xenopus laevis*. *Dev. Dyn.* 238: 3185-3192.

Pubmed: [Author and Title](#)

CrossRef: [Author and Title](#)

Google Scholar: [Author Only](#) [Title Only](#) [Author and Title](#)

Bemer, M. and Grossniklaus, U. (2012). Dynamic regulation of Polycomb group activity during plant development. *Curr. Opin. Plant Biol.* 15: 523-529.

Pubmed: [Author and Title](#)

CrossRef: [Author and Title](#)

Google Scholar: [Author Only](#) [Title Only](#) [Author and Title](#)

Benfey, P.N. and scheres, B. (2000). Root development. *Curr. Biol.* 10: R813-5.

Pubmed: [Author and Title](#)

CrossRef: [Author and Title](#)

Google Scholar: [Author Only](#) [Title Only](#) [Author and Title](#)

Birnbaum, K., Shasha, D.E., Wang, J.Y., and Jung, J.W. (2003). A gene expression map of the Arabidopsis root. *Science*.

Pubmed: [Author and Title](#)

CrossRef: [Author and Title](#)

Google Scholar: [Author Only](#) [Title Only](#) [Author and Title](#)

Bouyer, D., Roudier, F., Heese, M., Andersen, E.D., Gey, D., Nowack, M.K., Goodrich, J., Renou, J.-P., Grini, P.E., Colot, V., and Schnittger, A. (2011). Polycomb Repressive Complex 2 Controls the Embryo-to-Seedling Phase Transition. *PLoS Genet* 7: e1002014.

Pubmed: [Author and Title](#)

CrossRef: [Author and Title](#)

Google Scholar: [Author Only](#) [Title Only](#) [Author and Title](#)

Bracken, A.P., Pasini, D., Capra, M., Prosperini, E., Colli, E., and Helin, K. (2003). EZH2 is downstream of the pRB-E2F pathway, essential for proliferation and amplified in cancer. *The EMBO Journal* 22: 5323-5335.

Pubmed: [Author and Title](#)

CrossRef: [Author and Title](#)

Google Scholar: [Author Only](#) [Title Only](#) [Author and Title](#)

Brady, S.M. et al. (2011). A stele-enriched gene regulatory network in the Arabidopsis root. *Molecular Systems Biology* 7: 459.

Pubmed: [Author and Title](#)

CrossRef: [Author and Title](#)

Google Scholar: [Author Only](#) [Title Only](#) [Author and Title](#)

Brady, S.M., Orlando, D.A., Lee, J.Y., Wang, J.Y., Koch, J., Dinneny, J.R., Mace, D., Ohler, U., and Benfey, P.N. (2007). A High-Resolution Root Spatiotemporal Map Reveals Dominant Expression Patterns. *Science* 318: 801-806.

Pubmed: [Author and Title](#)

CrossRef: [Author and Title](#)

Google Scholar: [Author Only](#) [Title Only](#) [Author and Title](#)

Bruno, L., Muto, A., Spadafora, N.D., Iaria, D., Chiappetta, A., Van Lijsebettens, M., and Bitonti, M.B. (2011). Multi-probe in situ hybridization to whole mount Arabidopsis seedlings. *Int. J. Dev. Biol.* 55: 197-203.

Pubmed: [Author and Title](#)

CrossRef: [Author and Title](#)

Google Scholar: [Author Only](#) [Title Only](#) [Author and Title](#)

Chanvivattana, Y., Bishopp, A., Schubert, D., Stock, C., Moon, Y.-H., Sung, Z.R., and Goodrich, J. (2004). Interaction of Polycomb-group proteins controlling flowering in Arabidopsis. *Development* 131: 5263-5276.

Pubmed: [Author and Title](#)

CrossRef: [Author and Title](#)

Google Scholar: [Author Only](#) [Title Only](#) [Author and Title](#)

Ciferri, C., Lander, G.C., Maiolica, A., Herzog, F., Aebersold, R., and Nogales, E. (2012). Molecular architecture of human polycomb repressive complex 2. *Elife* 1: e00005.

Pubmed: [Author and Title](#)

CrossRef: [Author and Title](#)

Google Scholar: [Author Only](#) [Title Only](#) [Author and Title](#)

Clough, S.J. and Bent, A.F. (1998). Floral dip: a simplified method for *Agrobacterium*-mediated transformation of *Arabidopsis thaliana*. *The Plant Journal*.

Pubmed: [Author and Title](#)
CrossRef: [Author and Title](#)
Google Scholar: [Author Only](#) [Title Only](#) [Author and Title](#)

Coego, A., Brizuela, E., Castillejo, P., Ruiz, S., Koncz, C., Del Pozo, J.C., Pineiro, M., Jarillo, J.A., Paz-Ares, J., León, J., The TRANSPLANTA Consortium (2014). The TRANSPLANTA collection of Arabidopsis lines: a resource for functional analysis of transcription factors based on their conditional overexpression. The Plant Journal.

Pubmed: [Author and Title](#)
CrossRef: [Author and Title](#)
Google Scholar: [Author Only](#) [Title Only](#) [Author and Title](#)

De Lucia, F., Crevillen, P., Jones, A.M.E., Greb, T., and Dean, C. (2008). A PHD-polycomb repressive complex 2 triggers the epigenetic silencing of FLC during vernalization. Proceedings of the National Academy of Sciences 105: 16831-16836.

Pubmed: [Author and Title](#)
CrossRef: [Author and Title](#)
Google Scholar: [Author Only](#) [Title Only](#) [Author and Title](#)

De Rybel, B. et al. (2014). Integration of growth and patterning during vascular tissue formation in Arabidopsis. Science 345: 1255215-1255215.

Pubmed: [Author and Title](#)
CrossRef: [Author and Title](#)
Google Scholar: [Author Only](#) [Title Only](#) [Author and Title](#)

Deal, R.B. and Henikoff, S. (2010). A Simple Method for Gene Expression and Chromatin Profiling of Individual Cell Types within a Tissue. Developmental Cell 18: 1030-1040.

Pubmed: [Author and Title](#)
CrossRef: [Author and Title](#)
Google Scholar: [Author Only](#) [Title Only](#) [Author and Title](#)

Deng, W., Buzas, D.M., Ying, H., Robertson, M., Taylor, J., Peacock, W.J., Dennis, E.S., and Helliwell, C. (2013). Arabidopsis Polycomb Repressive Complex 2 binding sites contain putative GAGA factor binding motifs within coding regions of genes. BMC Genomics 14: 593.

Pubmed: [Author and Title](#)
CrossRef: [Author and Title](#)
Google Scholar: [Author Only](#) [Title Only](#) [Author and Title](#)

Derkacheva, M., Steinbach, Y., Wildhaber, T., Mozhgová, I., Mahrez, W., Nanni, P., Bischof, S., Grisse, W., and Hennig, L. (2013). Arabidopsis MSI1 connects LHP1 to PRC2 complexes. The EMBO Journal.

Pubmed: [Author and Title](#)
CrossRef: [Author and Title](#)
Google Scholar: [Author Only](#) [Title Only](#) [Author and Title](#)

Dolan, L., Janmaat, K., Willemsen, V., Linstead, P., Poethig, S., Roberts, K., and scheres, B. (1993). Cellular organisation of the Arabidopsis thaliana root. Development 119: 71-84.

Pubmed: [Author and Title](#)
CrossRef: [Author and Title](#)
Google Scholar: [Author Only](#) [Title Only](#) [Author and Title](#)

Du, Z., Zhou, X., Ling, Y., Zhang, Z., and Su, Z. (2010). agriGO: a GO analysis toolkit for the agricultural community. Nucleic Acids Res. 38: W64-70.

Pubmed: [Author and Title](#)
CrossRef: [Author and Title](#)
Google Scholar: [Author Only](#) [Title Only](#) [Author and Title](#)

Etchells, J.P. and Turner, S.R. (2010). Orientation of vascular cell divisions in Arabidopsis. Plant Signal Behav 5: 730-732.

Pubmed: [Author and Title](#)
CrossRef: [Author and Title](#)
Google Scholar: [Author Only](#) [Title Only](#) [Author and Title](#)

Etchells, J.P., Provost, C.M., Mishra, L., and Turner, S.R. (2013). WOX4 and WOX14 act downstream of the PXY receptor kinase to regulate plant vascular proliferation independently of any role in vascular organisation. Development 140: 2224-2234.

Pubmed: [Author and Title](#)
CrossRef: [Author and Title](#)
Google Scholar: [Author Only](#) [Title Only](#) [Author and Title](#)

Fasano, C.A., Dimos, J.T., Ivanova, N.B., Lowry, N., Lemischka, I.R., and Temple, S. (2007). shRNA knockdown of Brni-1 reveals a critical role for p21-Rb pathway in NSC self-renewal during development. Cell Stem Cell 1: 87-99.

Pubmed: [Author and Title](#)
CrossRef: [Author and Title](#)
Google Scholar: [Author Only](#) [Title Only](#) [Author and Title](#)

Fisher, K. and Turner, S. (2007). PXY, a receptor-like kinase essential for maintaining polarity during plant vascular-tissue development. Curr. Biol. 17: 1061-1066.

Pubmed: [Author and Title](#)
CrossRef: [Author and Title](#)
Google Scholar: [Author Only](#) [Title Only](#) [Author and Title](#)

Fu, C., Donovan, W.P., Shikapwashya-Hasser, O., Ye, X., and Cole, R.H. (2014). Hot Fusion: An Efficient Method to Clone Multiple DNA Fragments as Well as Inverted Repeats without Ligase. PLoS ONE 9: e115318.

Pubmed: [Author and Title](#)

CrossRef: [Author and Title](#)
Google Scholar: [Author Only](#) [Title Only](#) [Author and Title](#)

Gaudinier, A. et al. (2011). Enhanced Y1H assays for Arabidopsis. Nat Meth 8: 1053-1055.

Pubmed: [Author and Title](#)
CrossRef: [Author and Title](#)
Google Scholar: [Author Only](#) [Title Only](#) [Author and Title](#)

Gu, X., Xu, T., and He, Y. (2014). A histone H3 lysine-27 methyltransferase complex represses lateral root formation in Arabidopsis thaliana. Molecular Plant 7: 977-988.

Pubmed: [Author and Title](#)
CrossRef: [Author and Title](#)
Google Scholar: [Author Only](#) [Title Only](#) [Author and Title](#)

He, C., Chen, X., Huang, H., and Xu, L. (2012). Reprogramming of H3K27me3 Is Critical for Acquisition of Pluripotency from Cultured Arabidopsis Tissues. PLoS Genet 8: e1002911.

Pubmed: [Author and Title](#)
CrossRef: [Author and Title](#)
Google Scholar: [Author Only](#) [Title Only](#) [Author and Title](#)

Helin, K. and Dhanak, D. (2013). Chromatin proteins and modifications as drug targets. Nature 502: 480-488.

Pubmed: [Author and Title](#)
CrossRef: [Author and Title](#)
Google Scholar: [Author Only](#) [Title Only](#) [Author and Title](#)

Hellens, R.P., Edwards, E.A., Leyland, N.R., Bean, S., and Mullineaux, P.M. (2000). pGreen: a versatile and flexible binary Ti vector for Agrobacterium-mediated plant transformation. Plant Mol Biol 42: 819-832.

Pubmed: [Author and Title](#)
CrossRef: [Author and Title](#)
Google Scholar: [Author Only](#) [Title Only](#) [Author and Title](#)

Hennig, L. and Derkacheva, M. (2009). Diversity of Polycomb group complexes in plants: same rules, different players? Trends in Genetics 25: 414-423.

Pubmed: [Author and Title](#)
CrossRef: [Author and Title](#)
Google Scholar: [Author Only](#) [Title Only](#) [Author and Title](#)

Hennig, L., Taranto, P., Walser, M., Schönrock, N., and Grissem, W. (2003). Arabidopsis MSI1 is required for epigenetic maintenance of reproductive development. Development 130: 2555-2565.

Pubmed: [Author and Title](#)
CrossRef: [Author and Title](#)
Google Scholar: [Author Only](#) [Title Only](#) [Author and Title](#)

Hirabayashi, Y., Suzuki, N., Tsuboi, M., Endo, T.A., Toyoda, T., Shinga, J., Koseki, H., Vidal, M., and Gotoh, Y. (2009). Polycomb limits the neurogenic competence of neural precursor cells to promote astrogenic fate transition. Neuron 63: 600-613.

Pubmed: [Author and Title](#)
CrossRef: [Author and Title](#)
Google Scholar: [Author Only](#) [Title Only](#) [Author and Title](#)

Ikeuchi, M. et al. (2015). PRC2 represses dedifferentiation of mature somatic cells in Arabidopsis. Nature Plants 1: 15089.

Pubmed: [Author and Title](#)
CrossRef: [Author and Title](#)
Google Scholar: [Author Only](#) [Title Only](#) [Author and Title](#)

Inoue, T., Higuchi, M., Hashimoto, Y., Seki, M., Kobayashi, M., Kato, T., Tabata, S., Shinozaki, K., and Kakimoto, T. (2001). Identification of CRE1 as a cytokinin receptor from Arabidopsis. Nature 409: 1060-1063.

Pubmed: [Author and Title](#)
CrossRef: [Author and Title](#)
Google Scholar: [Author Only](#) [Title Only](#) [Author and Title](#)

Jullien, P.E., Mosquana, A., Ingouff, M., Sakata, T., Ohad, N., and Berger, F. (2008). Retinoblastoma and its binding partner MSI1 control imprinting in Arabidopsis. Plos Biol 6: e194.

Pubmed: [Author and Title](#)
CrossRef: [Author and Title](#)
Google Scholar: [Author Only](#) [Title Only](#) [Author and Title](#)

Karimi, M., De Meyer, B., and Hilson, P. (2005). Modular cloning in plant cells. Trends in Plant Science.

Pubmed: [Author and Title](#)
CrossRef: [Author and Title](#)
Google Scholar: [Author Only](#) [Title Only](#) [Author and Title](#)

Kinoshita, T., Harada, J.J., Goldberg, R.B., and Fischer, R.L. (2001). Polycomb repression of flowering during early plant development. Proc. Natl. Acad. Sci. U.S.A 98: 14156-14161.

Pubmed: [Author and Title](#)
CrossRef: [Author and Title](#)
Google Scholar: [Author Only](#) [Title Only](#) [Author and Title](#)

Kleer, C.G. et al. (2003). EZH2 is a marker of aggressive breast cancer and promotes neoplastic transformation of breast epithelial cells. Proc. Natl. Acad. Sci. U.S.A 100: 11606-11611.

Pubmed: [Author and Title](#)
CrossRef: [Author and Title](#)

Google Scholar: [Author Only](#) [Title Only](#) [Author and Title](#)

Köhler, C., Hennig, L., Bouveret, R., Gheyselinck, J., Grossniklaus, U., and Gruissem, W. (2003). Arabidopsis MSI1 is a component of the MEA/FIE Polycomb group complex and required for seed development. The EMBO Journal 22: 4804-4814.

Pubmed: [Author and Title](#)

CrossRef: [Author and Title](#)

Google Scholar: [Author Only](#) [Title Only](#) [Author and Title](#)

Köhler, C., Page, D.R., Gagliardini, V., and Grossniklaus, U. (2005). The Arabidopsis thaliana MEDEA Polycomb group protein controls expression of PHERES1 by parental imprinting. Nat Genet 37: 28-30.

Pubmed: [Author and Title](#)

CrossRef: [Author and Title](#)

Google Scholar: [Author Only](#) [Title Only](#) [Author and Title](#)

Kubo, M. (2005). Transcription switches for protoxylem and metaxylem vessel formation. Genes & Development 19: 1855-1860.

Pubmed: [Author and Title](#)

CrossRef: [Author and Title](#)

Google Scholar: [Author Only](#) [Title Only](#) [Author and Title](#)

Kumar, R., Ichihashi, Y., Kimura, S., Chitwood, D.H., Headland, L.R., Peng, J., Maloof, J.N., and Sinha, N.R. (2012). A high-throughput method for Illumina RNA-Seq library preparation. Front Plant Sci 3.

Pubmed: [Author and Title](#)

CrossRef: [Author and Title](#)

Google Scholar: [Author Only](#) [Title Only](#) [Author and Title](#)

Kuzmichev, A., Margueron, R., Vaquero, A., Preissner, T.S., Scher, M., Kirmizis, A., Ouyang, X., Brockdorff, N., Abate-Shen, C., Farnham, P., and Reinberg, D. (2005). Composition and histone substrates of polycomb repressive group complexes change during cellular differentiation. Proc. Natl. Acad. Sci. U.S.A. 102: 1859-1864.

Pubmed: [Author and Title](#)

CrossRef: [Author and Title](#)

Google Scholar: [Author Only](#) [Title Only](#) [Author and Title](#)

Lafos, M., Kroll, P., Hohenstatt, M.L., Thorpe, F.L., Clarenz, O., and Schubert, D. (2011). Dynamic regulation of H3K27 trimethylation during Arabidopsis differentiation. PLoS Genet 7: e1002040.

Pubmed: [Author and Title](#)

CrossRef: [Author and Title](#)

Google Scholar: [Author Only](#) [Title Only](#) [Author and Title](#)

Langmead, B., Trapnell, C., Pop, M., and Salzberg, S.L. (2009). Ultrafast and memory-efficient alignment of short DNA sequences to the human genome. Genome Biol 10: R25.

Pubmed: [Author and Title](#)

CrossRef: [Author and Title](#)

Google Scholar: [Author Only](#) [Title Only](#) [Author and Title](#)

Laugesen, A and Helin, K. (2014). Chromatin repressive complexes in stem cells, development, and cancer. Cell Stem Cell 14: 735-751.

Pubmed: [Author and Title](#)

CrossRef: [Author and Title](#)

Google Scholar: [Author Only](#) [Title Only](#) [Author and Title](#)

Lee, J.-Y., Colinas, J., Wang, J.Y., Mace, D., Ohler, U., and Benfey, P.N. (2006). Transcriptional and posttranscriptional regulation of transcription factor expression in Arabidopsis roots. Proc. Natl. Acad. Sci. U.S.A. 103: 6055-6060.

Pubmed: [Author and Title](#)

CrossRef: [Author and Title](#)

Google Scholar: [Author Only](#) [Title Only](#) [Author and Title](#)

Ma, S., Shah, S., Bohnert, H.J., Snyder, M., and Dinesh-Kumar, S.P. (2013). Incorporating motif analysis into gene co-expression networks reveals novel modular expression pattern and new signaling pathways. PLoS Genet 9: e1003840.

Pubmed: [Author and Title](#)

CrossRef: [Author and Title](#)

Google Scholar: [Author Only](#) [Title Only](#) [Author and Title](#)

Mahonen, A.P. (2000). A novel two-component hybrid molecule regulates vascular morphogenesis of the Arabidopsis root. Genes & Development 14: 2938-2943.

Pubmed: [Author and Title](#)

CrossRef: [Author and Title](#)

Google Scholar: [Author Only](#) [Title Only](#) [Author and Title](#)

Mahonen, A.P. (2006). Cytokinin Signaling and Its Inhibitor AHP6 Regulate Cell Fate During Vascular Development. Science 311: 94-98.

Pubmed: [Author and Title](#)

CrossRef: [Author and Title](#)

Google Scholar: [Author Only](#) [Title Only](#) [Author and Title](#)

Mallory, A.C. (2005). MicroRNA-Directed Regulation of Arabidopsis AUXIN RESPONSE FACTOR17 Is Essential for Proper Development and Modulates Expression of Early Auxin Response Genes. THE PLANT CELL ONLINE 17: 1360-1375.

Pubmed: [Author and Title](#)

CrossRef: [Author and Title](#)

Google Scholar: [Author Only](#) [Title Only](#) [Author and Title](#)

Margueron, R. and Reinberg, D. (2011). The Polycomb complex PRC2 and its mark in life. Nature 469: 343-349.

Pubmed: [Author and Title](#)
CrossRef: [Author and Title](#)
Google Scholar: [Author Only](#) [Title Only](#) [Author and Title](#)

Margueron, R., Li, G., Sarma, K., Blais, A., Zavadil, J., Woodcock, C.L., Dynlacht, B.D., and Reinberg, D. (2008). Ezh1 and Ezh2 maintain repressive chromatin through different mechanisms. *Molecular Cell* 32: 503-518.

Pubmed: [Author and Title](#)
CrossRef: [Author and Title](#)
Google Scholar: [Author Only](#) [Title Only](#) [Author and Title](#)

Mozgová, I. and Hennig, L. (2015). The Polycomb Group Protein Regulatory Network. <http://dx.doi.org/10.1146/annurev-arplant-043014-115627>.

Pubmed: [Author and Title](#)
CrossRef: [Author and Title](#)
Google Scholar: [Author Only](#) [Title Only](#) [Author and Title](#)

Nakagawa, T., Kurose, T., Hino, T., Tanaka, K., Kawamukai, M., Niwa, Y., Toyooka, K., Matsuoka, K., Jinbo, T., and Kimura, T. (2007). Development of series of gateway binary vectors, pGWBs, for realizing efficient construction of fusion genes for plant transformation. *J. Biosci. Bioeng.* 104: 34-41.

Pubmed: [Author and Title](#)
CrossRef: [Author and Title](#)
Google Scholar: [Author Only](#) [Title Only](#) [Author and Title](#)

Ohno, K., McCabe, D., Czermin, B., Imhof, A., and Pirrotta, V. (2008). ESC, ESCL and their roles in Polycomb Group mechanisms. *Mech. Dev.* 125: 527-541.

Pubmed: [Author and Title](#)
CrossRef: [Author and Title](#)
Google Scholar: [Author Only](#) [Title Only](#) [Author and Title](#)

Okushima, Y. (2005). Functional Genomic Analysis of the AUXIN RESPONSE FACTOR Gene Family Members in *Arabidopsis thaliana*: Unique and Overlapping Functions of ARF7 and ARF19. *The Plant Cell* 17: 444-463.

Pubmed: [Author and Title](#)
CrossRef: [Author and Title](#)
Google Scholar: [Author Only](#) [Title Only](#) [Author and Title](#)

Ossowski, S., Schwab, R., and Weigel, D. (2008). Gene silencing in plants using artificial microRNAs and other small RNAs. *The Plant Journal* 53: 674-690.

Pubmed: [Author and Title](#)
CrossRef: [Author and Title](#)
Google Scholar: [Author Only](#) [Title Only](#) [Author and Title](#)

Pasini, D., Bracken, A.P., Hansen, J.B., Capillo, M., and Helin, K. (2007). The polycomb group protein Suz12 is required for embryonic stem cell differentiation. *Mol. Cell. Biol.* 27: 3769-3779.

Pubmed: [Author and Title](#)
CrossRef: [Author and Title](#)
Google Scholar: [Author Only](#) [Title Only](#) [Author and Title](#)

Quinlan, A.R. and Hall, I.M. (2010). BEDTools: a flexible suite of utilities for comparing genomic features. *Bioinformatics* 26: 841-842.

Pubmed: [Author and Title](#)
CrossRef: [Author and Title](#)
Google Scholar: [Author Only](#) [Title Only](#) [Author and Title](#)

Rademacher, E.H., Möller, B., Lokerse, A.S., Llavata-Peris, C.I., van den Berg, W., and Weijers, D. (2011). A cellular expression map of the *Arabidopsis* AUXIN RESPONSE FACTOR gene family. *The Plant Journal* 68: 597-606.

Pubmed: [Author and Title](#)
CrossRef: [Author and Title](#)
Google Scholar: [Author Only](#) [Title Only](#) [Author and Title](#)

Reece-Hoyes, J.S. et al. (2011). Yeast one-hybrid assays for gene-centered human gene regulatory network mapping. *Nat Meth* 8: 1050-1052.

Pubmed: [Author and Title](#)
CrossRef: [Author and Title](#)
Google Scholar: [Author Only](#) [Title Only](#) [Author and Title](#)

Roudier, F. et al. (2011). Integrative epigenomic mapping defines four main chromatin states in *Arabidopsis*. *The EMBO Journal* 30: 1928-1938.

Pubmed: [Author and Title](#)
CrossRef: [Author and Title](#)
Google Scholar: [Author Only](#) [Title Only](#) [Author and Title](#)

Rueda-Romero, P., Barrero-Sicilia, C., Gómez-Cadenas, A., Carbonero, P., and Oñate-Sánchez, L. (2012). *Arabidopsis thaliana* DOF6 negatively affects germination in non-after-ripened seeds and interacts with TCP14. *Journal of Experimental Botany* 63: 1937-1949.

Pubmed: [Author and Title](#)
CrossRef: [Author and Title](#)
Google Scholar: [Author Only](#) [Title Only](#) [Author and Title](#)

Scheres, B. (2007). Stem-cell niches: nursery rhymes across kingdoms. *Nature Reviews Molecular Cell Biology* 8: 345-354.

Pubmed: [Author and Title](#)

CrossRef: [Author and Title](#)
Google Scholar: [Author Only](#) [Title Only](#) [Author and Title](#)

Shahram Emami, M.-C.Y.J.R.D. (2013). A robust family of Golden Gate Agrobacterium vectors for plant synthetic biology. Front Plant Sci 4.

Pubmed: [Author and Title](#)
CrossRef: [Author and Title](#)
Google Scholar: [Author Only](#) [Title Only](#) [Author and Title](#)

Shannon, P., Markiel, A., Ozier, O., Baliga, N.S., Wang, J.T., Ramage, D., Amin, N., Schwikowski, B., and Ideker, T. (2003). Cytoscape: a software environment for integrated models of biomolecular interaction networks. Genome Research 13: 2498-2504.

Pubmed: [Author and Title](#)
CrossRef: [Author and Title](#)
Google Scholar: [Author Only](#) [Title Only](#) [Author and Title](#)

She, W., Grimanelli, D., and Baroux, C. (2014). An efficient method for quantitative, single-cell analysis of chromatin modification and nuclear architecture in whole-mount ovules in Arabidopsis. J Vis Exp: e51530.

Pubmed: [Author and Title](#)
CrossRef: [Author and Title](#)
Google Scholar: [Author Only](#) [Title Only](#) [Author and Title](#)

Sher, F., Rössler, R., Brouwer, N., Balasubramanian, V., Boddeke, E., and Copray, S. (2008). Differentiation of neural stem cells into oligodendrocytes: involvement of the polycomb group protein Ezh2. Stem Cells 26: 2875-2883.

Pubmed: [Author and Title](#)
CrossRef: [Author and Title](#)
Google Scholar: [Author Only](#) [Title Only](#) [Author and Title](#)

Sieburth, L.E. and Meyerowitz, E.M. (1997). Molecular dissection of the AGAMOUS control region shows that cis elements for spatial regulation are located intragenically. The Plant Cell 9: 355-365.

Pubmed: [Author and Title](#)
CrossRef: [Author and Title](#)
Google Scholar: [Author Only](#) [Title Only](#) [Author and Title](#)

Stojic, L. et al. (2011). Chromatin regulated interchange between polycomb repressive complex 2 (PRC2)-Ezh2 and PRC2-Ezh1 complexes controls myogenin activation in skeletal muscle cells. Epigenetics Chromatin 4: 16.

Pubmed: [Author and Title](#)
CrossRef: [Author and Title](#)
Google Scholar: [Author Only](#) [Title Only](#) [Author and Title](#)

Takawa, M. et al. (2011). Validation of the histone methyltransferase EZH2 as a therapeutic target for various types of human cancer and as a prognostic marker. Cancer Sci. 102: 1298-1305.

Pubmed: [Author and Title](#)
CrossRef: [Author and Title](#)
Google Scholar: [Author Only](#) [Title Only](#) [Author and Title](#)

Taylor-Teeple, M. et al. (2015). An Arabidopsis gene regulatory network for secondary cell wall synthesis. Nature 517: 571-575.

Pubmed: [Author and Title](#)
CrossRef: [Author and Title](#)
Google Scholar: [Author Only](#) [Title Only](#) [Author and Title](#)

Terpstra, I. and Heidstra, R. (2009). Stem cells: The root of all cells. Seminars in Cell & Developmental Biology 20: 1089-1096.

Pubmed: [Author and Title](#)
CrossRef: [Author and Title](#)
Google Scholar: [Author Only](#) [Title Only](#) [Author and Title](#)

Truernit, E., Bauby, H., Dubreucq, B., Grandjean, O., Runions, J., Barthelemy, J., and Palauqui, J.C. (2008). High-Resolution Whole-Mount Imaging of Three-Dimensional Tissue Organization and Gene Expression Enables the Study of Phloem Development and Structure in Arabidopsis. THE PLANT CELL ONLINE 20: 1494-1503.

Pubmed: [Author and Title](#)
CrossRef: [Author and Title](#)
Google Scholar: [Author Only](#) [Title Only](#) [Author and Title](#)

Turck, F., Roudier, F., Farrona, S., Martin-Magniette, M.-L., Guillaume, E., Buisine, N., Gagnot, S., Martienssen, R.A., Coupland, G., and Colot, V. (2007). Arabidopsis TFL2/LHP1 specifically associates with genes marked by trimethylation of histone H3 lysine 27. PLoS Genet 3: e86.

Pubmed: [Author and Title](#)
CrossRef: [Author and Title](#)
Google Scholar: [Author Only](#) [Title Only](#) [Author and Title](#)

Varambally, S., Dhanasekaran, S.M., Zhou, M., Barrette, T.R., Kumar-Sinha, C., Sanda, M.G., Ghosh, D., Pienta, K.J., Sewalt, R.G.A.B., Otte, A.P., Rubin, M.A., and Chinnaiyan, A.M. (2002). The polycomb group protein EZH2 is involved in progression of prostate cancer. Nature 419: 624-629.

Pubmed: [Author and Title](#)
CrossRef: [Author and Title](#)
Google Scholar: [Author Only](#) [Title Only](#) [Author and Title](#)

Wagener, N., Macher-Goeppinger, S., Pritsch, M., Hüsing, J., Hoppe-Seyler, K., Schirmacher, P., Pfizenmaier, J., Haferkamp, A., Hoppe-Seyler, F., and Hohenfellner, M. (2010). Enhancer of zeste homolog 2 (EZH2) expression is an independent prognostic factor in renal cell carcinoma. BMC Cancer 10: 524.

Pubmed: [Author and Title](#)

CrossRef: [Author and Title](#)
Google Scholar: [Author Only](#) [Title Only](#) [Author and Title](#)

Wang, D., Tyson, M.D., Jackson, S.S., and Yadegari, R. (2006). Partially redundant functions of two SET-domain polycomb-group proteins in controlling initiation of seed development in Arabidopsis. Proc. Natl. Acad. Sci. U.S.A 103: 13244-13249.

Pubmed: [Author and Title](#)
CrossRef: [Author and Title](#)
Google Scholar: [Author Only](#) [Title Only](#) [Author and Title](#)

Yadegari, R., Kinoshita, T., Lotan, O., Cohen, G., Katz, A., Choi, Y., Katz, A., Nakashima, K., Harada, J.J., Goldberg, R.B., Fischer, R.L., and Ohad, N. (2000). Mutations in the FIE and MEA genes that encode interacting polycomb proteins cause parent-of-origin effects on seed development by distinct mechanisms. The Plant Cell 12: 2367-2382.

Pubmed: [Author and Title](#)
CrossRef: [Author and Title](#)
Google Scholar: [Author Only](#) [Title Only](#) [Author and Title](#)

Yamaguchi, M., Ohtani, M., Mitsuda, N., Kubo, M., Ohme-Takagi, M., Fukuda, H., and Demura, T. (2010). VND-INTERACTING2, a NAC domain transcription factor, negatively regulates xylem vessel formation in Arabidopsis. THE PLANT CELL ONLINE 22: 1249-1263.

Pubmed: [Author and Title](#)
CrossRef: [Author and Title](#)
Google Scholar: [Author Only](#) [Title Only](#) [Author and Title](#)

Zhang, X., Clarenz, O., Cokus, S., Bernatavichute, Y.V., Pellegrini, M., Goodrich, J., and Jacobsen, S.E. (2007a). Whole-genome analysis of histone H3 lysine 27 trimethylation in Arabidopsis. Plos Biol 5: e129.

Pubmed: [Author and Title](#)
CrossRef: [Author and Title](#)
Google Scholar: [Author Only](#) [Title Only](#) [Author and Title](#)

Zhang, X., Germann, S., Blus, B.J., Khorasanizadeh, S., Gaudin, V., and Jacobsen, S.E. (2007b). The Arabidopsis LHP1 protein colocalizes with histone H3 Lys27 trimethylation. Nat. Struct. Mol. Biol. 14: 869-871.

Pubmed: [Author and Title](#)
CrossRef: [Author and Title](#)
Google Scholar: [Author Only](#) [Title Only](#) [Author and Title](#)

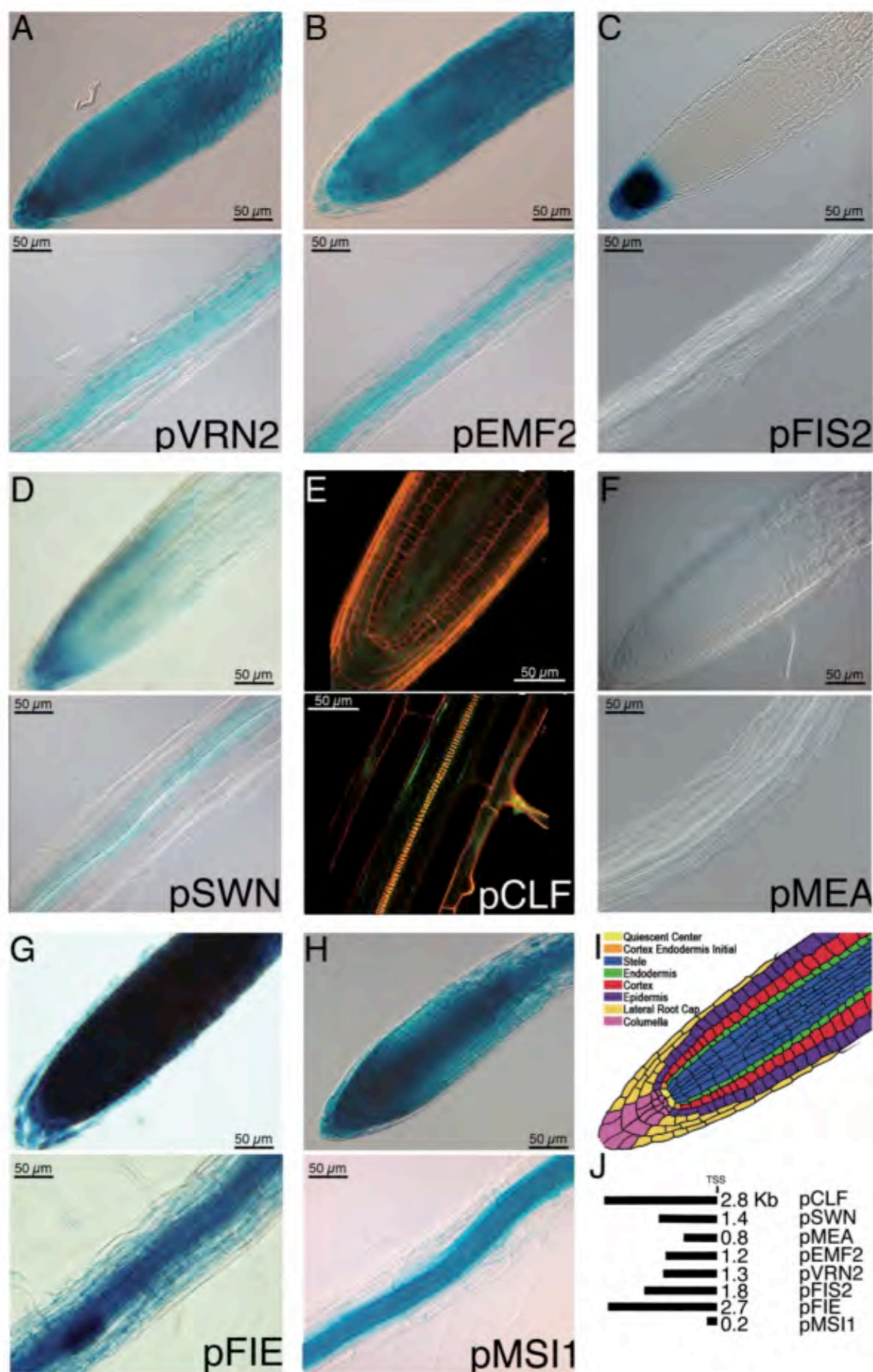


Figure 1. PRC2 genes are expressed in unique and overlapping cell types in the *Arabidopsis thaliana* root. For each genotype, the top panel shows the root meristem while the bottom panel shows the maturation/differentiation zone of the root. All images were taken under the same acquisition conditions. (A) VRN2pro:GUS expression. (B) EMF2pro:GUS expression. (C) FIS2pro:GUS expression. (D) SWNpro:GUS expression. (E) CLFpro:VenusN7 expression. (F) MEApro:GUS expression. (G) FIEpro:GUS expression. (H) MSI1pro:GUS expression. (I) Cartoon of the different cell types and tissues in the *Arabidopsis thaliana* root. (J) Promoter lengths of the different PRC2 genes used in the reporter lines. Translational start site = TSS.

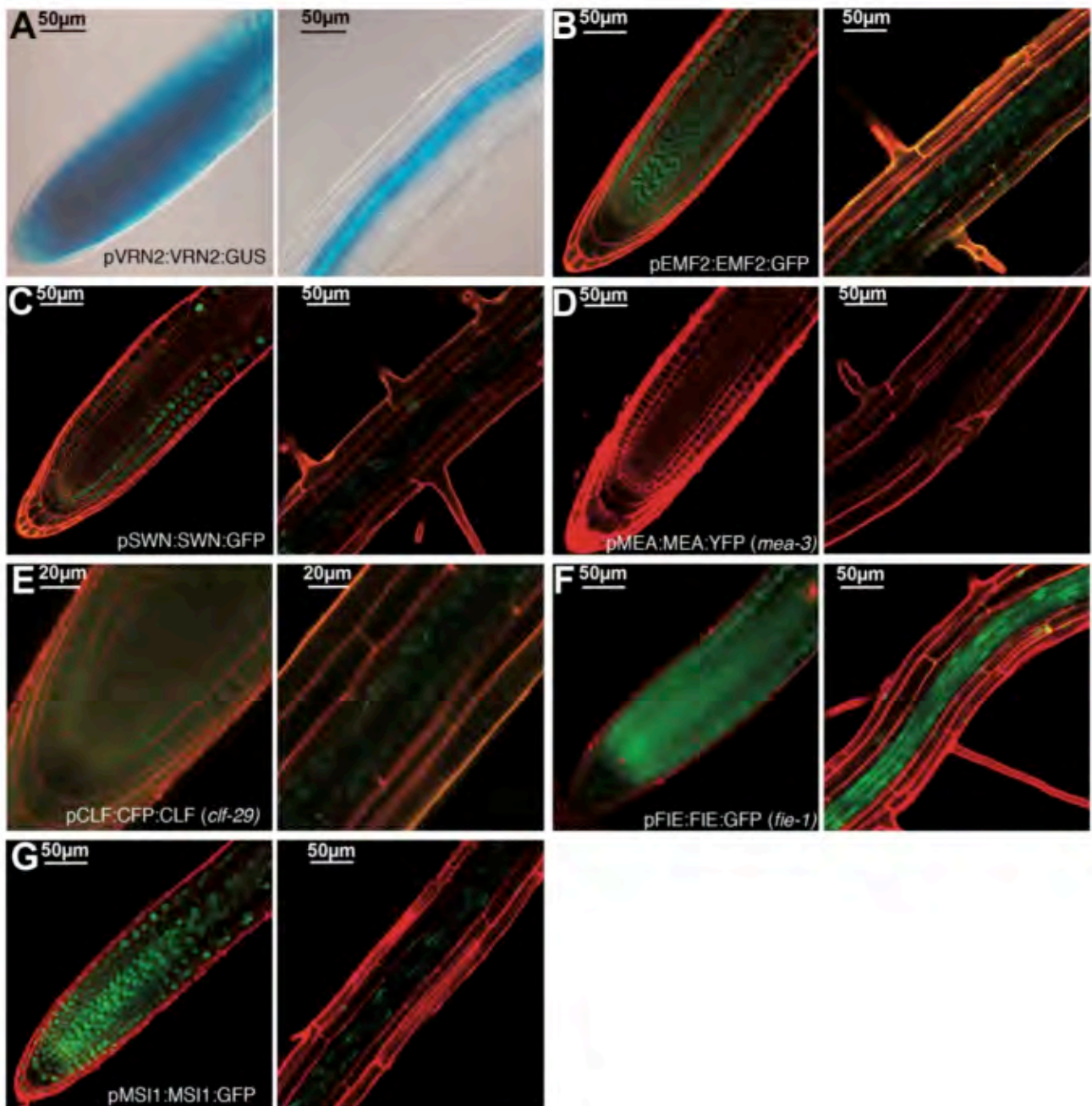


Figure 2: PRC2 proteins are found in unique and overlapping cell types in the *Arabidopsis thaliana* root. For each genotype, the left panel shows the root meristem while the right panel shows the maturation/differentiation zone of the root. (A) VRN2pro:VRN2:GUS (B) EMF2pro:EMF2:GFP (C) SWNpro:SWN:GFP (D) MEApro:MEA:YFP in *mea-3* (E) CLFpro:CLF:GFP in *clf-29*, (F) MSI1pro:MSI1:GFP (G) FIEpro:FIE:GFP in *fie-1*.

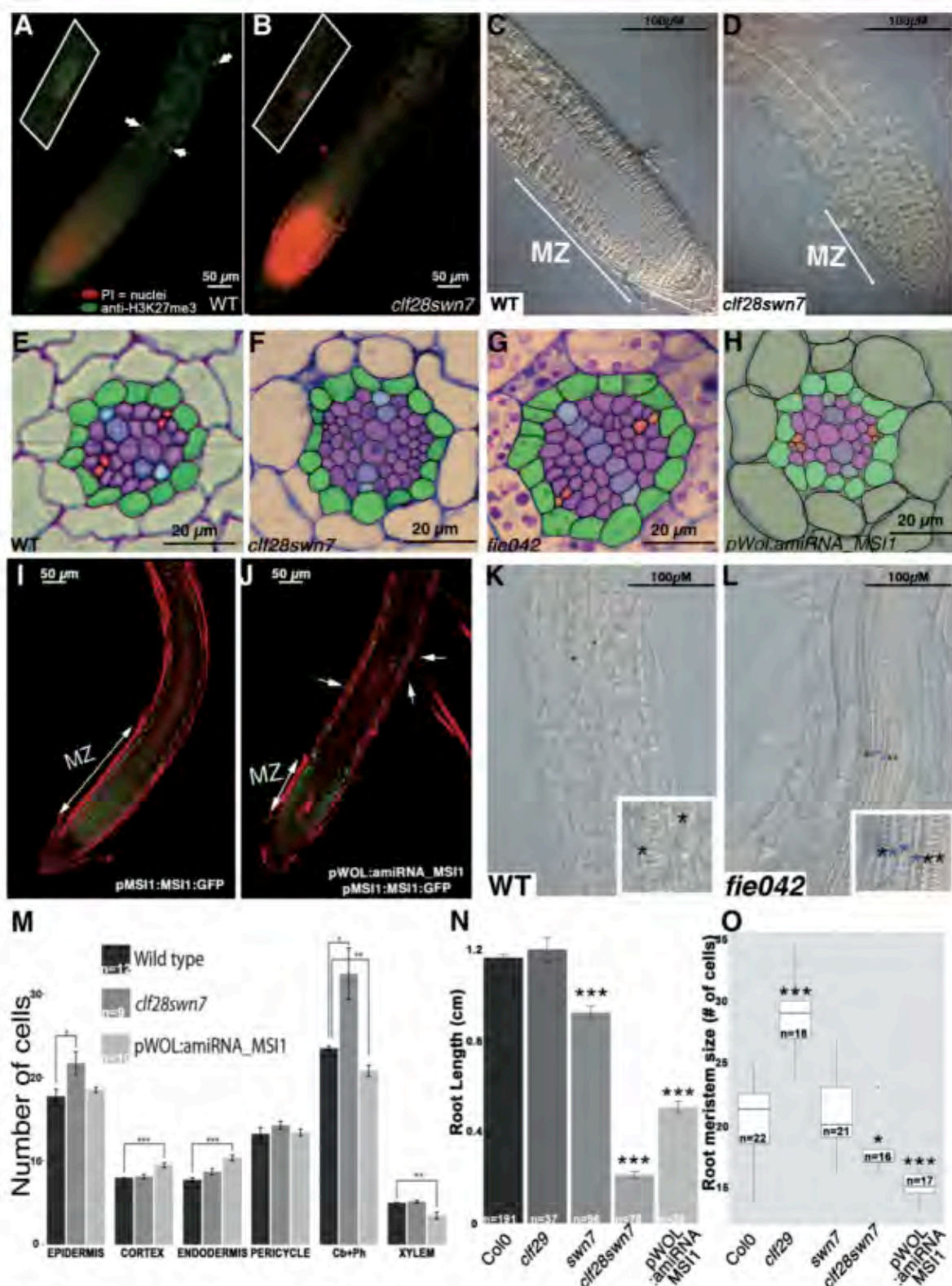


Figure 3: PRC2 regulates cell proliferation in the root meristem and vascular cylinder. (A-B) Whole mount immunostaining with antibodies specific for H3K27me3 (green in the wild-type Col-0) (A) and in the *clf-28 swn-7* double mutant (B). Nuclear staining is indicated with white arrows. A magnified nucleus is shown in the inset. (C-D) Differential Interference Contrast image of the root meristem of the wild-type Col-0 (C) and the *clf-28 swn-7* double mutant (D). White lines indicate the root meristematic zone (MZ). (E-H) Cross-sections showing the root vascular cylinder in wild-type Col-0 (E), *clf-28 swn-7* (F), *fie042* (G), and in the *WOLpro:amiRNA_MSI* line (H). Green indicates pericycle cells, purple indicates procambium cells, red/orange indicates phloem cells. (I-J) The MSI protein is expressed ubiquitously throughout the *Arabidopsis thaliana* root (I) but is depleted specifically from the vascular cylinder in the *WOLpro:amiRNA_MSI1* line in the *MSI1pro:MSI1:GFP* background (white arrows with one head) (J). Note the reduction in the length of the root meristem (white arrow with two heads). (K-L) Differential interference contrast image showing two protoxylem pole cell files (black asterisk) in the wild-type Col-0 (L) and ectopic protoxylem (black asterisk) and metaxylem (blue asterisk) in the *fie042* mutant background (L). (M) There are significantly more procambium and phloem and epidermal cells in the *clf-28 swn-7* mutant compared to wild-type Col-0. The reduction in MSI1 expression shows increased number of cortical and endodermal cells but lower levels of cells in the stele. (N) The roots of *swn-7*, *clf-28 swn-7* and *WOLpro:amiRNA_MSI* are significantly shorter than wild type Col-0 and *clf-29*. (O) There are more cells in the meristem of *clf-29* and fewer in *clf-28 swn-7* and *WOLpro:amiRNA_MSI* relative to wild type (Col-0). In all cases, significance was tested using a t-test. * = $p < .05$; ** = $p < .01$; *** = $p < .001$. Error bars indicate the standard error value.

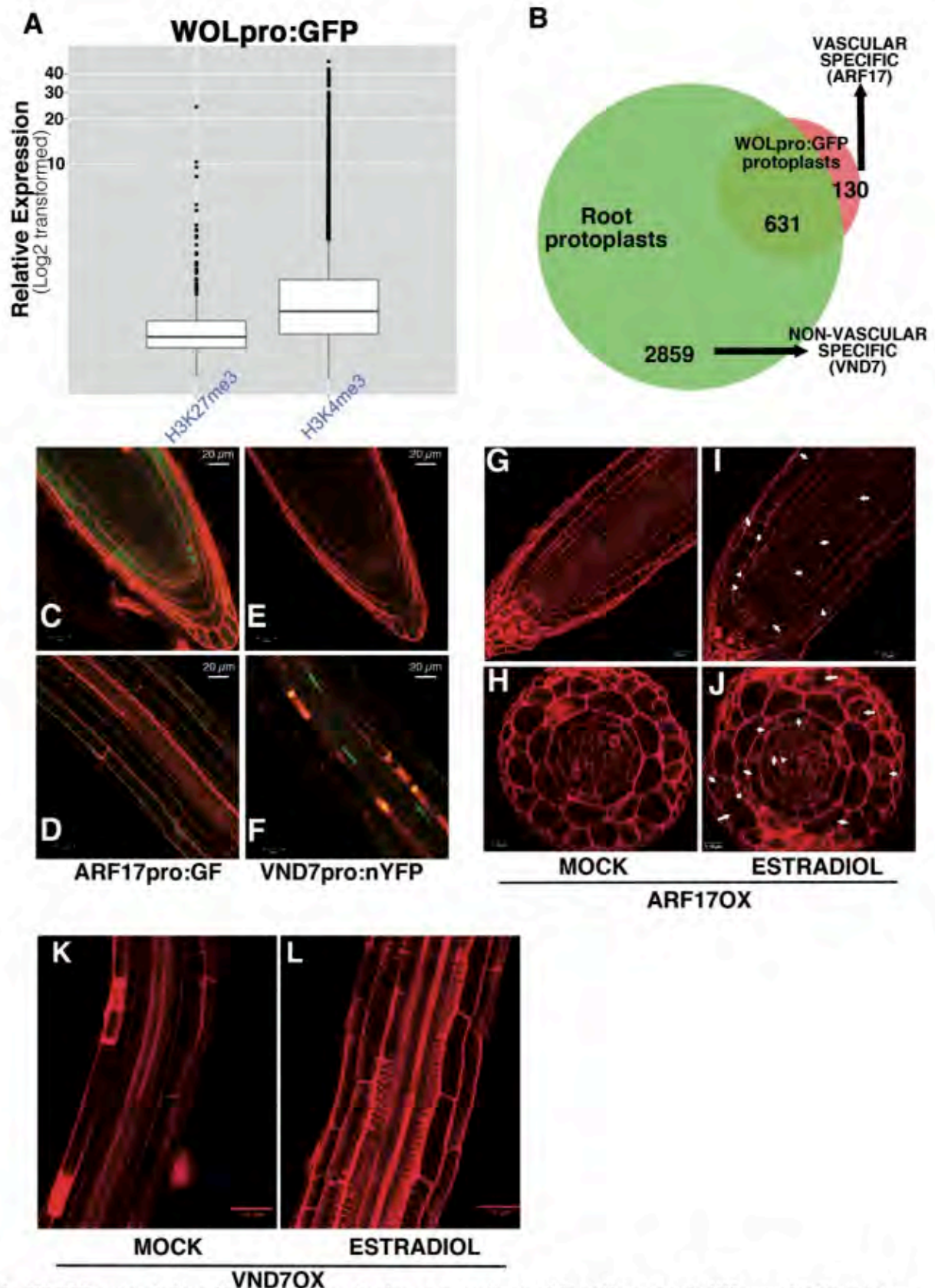


Figure 4. PRC2 regulates the balance between cell proliferation and differentiation in a tissue-specific manner in the *Arabidopsis thaliana* root. (A) Expression levels of genes marked by H3K27me3 in vascular cells relative to expression levels of genes marked by H3K4me3. Whole root and vascular-specific (pWOL:GFP positive) root protoplast were isolated by FACS and H3K27me3/H3K4me3 enriched regions were resolved by ChIPseq. Expression of the vascular specific H3K27me3 and H3K4me3 marked genes was determined using Brady et. al. 2007 transcriptional data. (B) Number of genes marked by H3K27me3 in non-vascular cells. (C-F) Expression of a gene marked specifically by H3K27me3 and not expressed in vascular cells (C,D) ARF17pro:GF and of a gene marked specifically by H3K27me3 and not expressed in non-vascular cells VND7pro:nYFP (E,F). (G-J) Estradiol induction of the ARF17 transcription factor results in small regions of additional cell proliferation in the vascular cylinder (I,J) compared to the mock-treated root (G,H). Asterisks indicate ectopic cell proliferation. (K-L) Estradiol induction of the VND7 transcription factor (L) results in ectopic xylem cell differentiation compared to a mock-treated root (K).

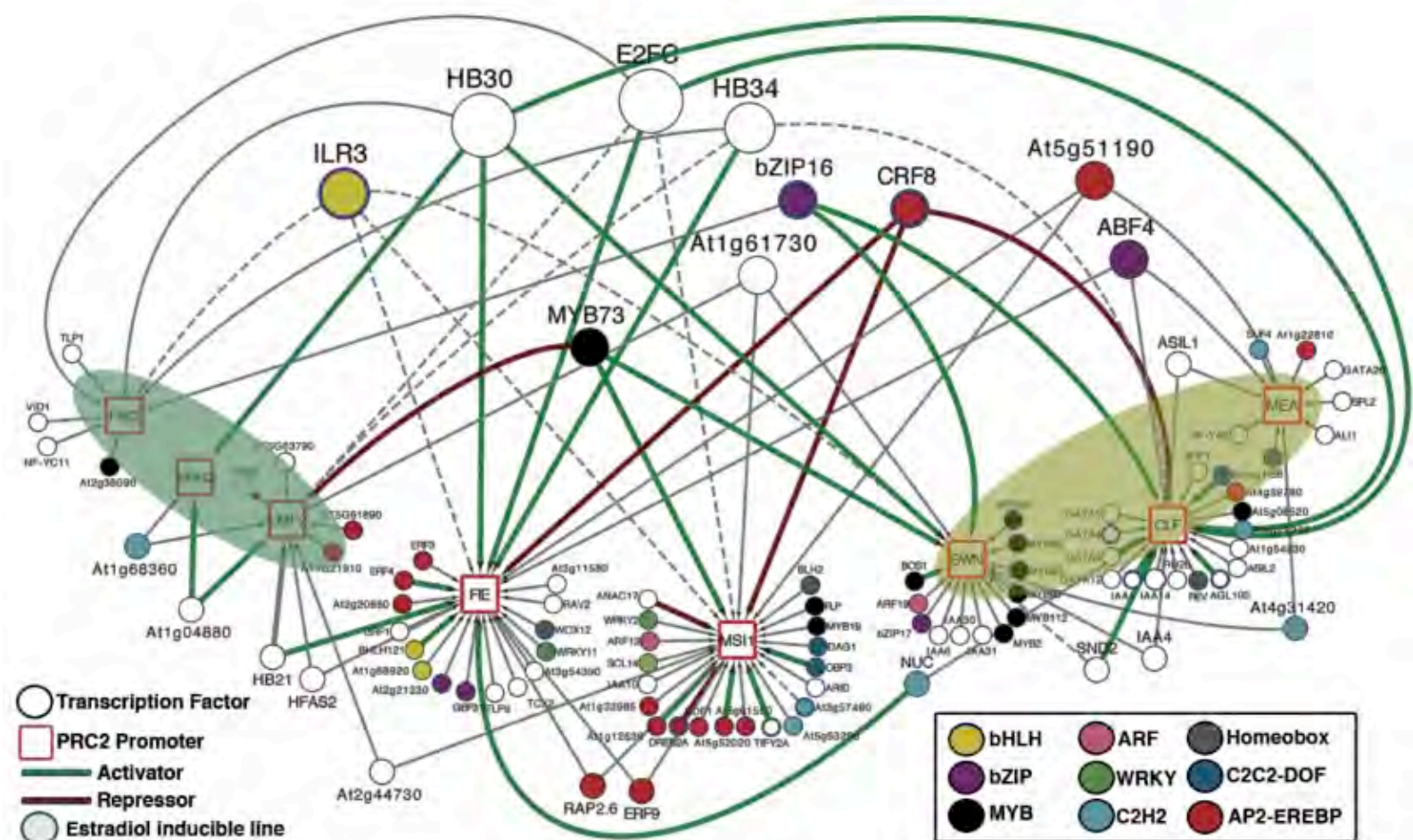


Figure 5. Transcription factors regulating PRC2 gene expression in planta. Squares represent PRC2 gene promoters, circles represent transcription factors. A line between a transcription factor and promoter indicates that an interaction was observed by yeast one hybrid. A green line or a red line indicates that the transcription factor has been validated in planta as activating or repressing, respectively, the target gene in planta in either a trans-activation assay or upon B-estradiol induction of the transcription factor. Transcription factors are additionally colored according to their respective family. Transcription factors that interact with the most PRC2 gene promoters are indicated at the top of the network, while transcription factors that interact with just a single promoter are located just beside their respective PRC2 gene promoter.

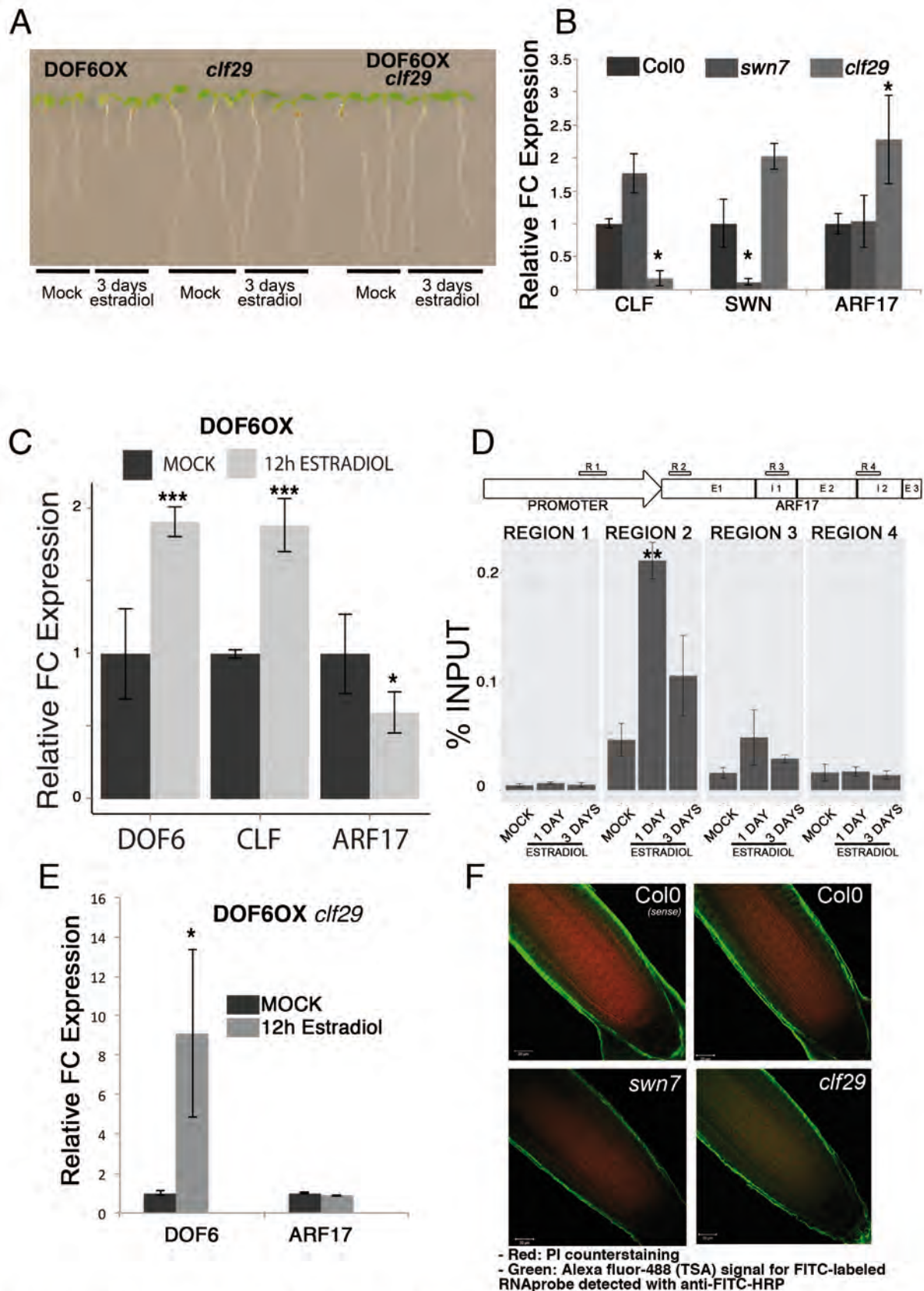


Figure 6. Functional validation of a multi-tier PRC2 gene regulatory network (TF → PRC2 gene → H3K27me3 regulated gene). (A) β -estradiol induction (3 days) of the DOF6 transcription factor results in a significantly shorter root. Root inhibition caused by the induction of DOF6 is abolished in the *clf29* background. (B) ARF17 expression is activated in the *clf-29* mutant. (C) Induction of DOF6 results in a significant increase in the amount of CLF expression and a corresponding repression of ARF17 expression, as revealed by RT-qPCR. (D) Induction of DOF6 results in a significant increase in H3K27me3 deposition in the ARF17 loci in the root tissue. (E) DOF6 induction does not affect ARF17 expression in the *clf-29* background. (F) Whole mount in-situ hybridization of ARF17 mRNA. ARF17 expression domain is expanded towards the vascular cylinder in the *clf-29* mutant. In all cases significance was tested using a t-test. * = $p < .05$; ** = $p < .01$; *** = $p < .001$. Error bars represent the standard error value of the log2 transformed expression. The mean is from 3 independent experiments (biological replicates), calculated from the average of 3 technical replicates per biological replicate. Each biological replicate captures expression from approximately 200 roots of each respective genotype. In each case the $\Delta\Delta Ct$ was calculated relative to an ubiquitin10 control.

Transcriptional Regulation of Arabidopsis Polycomb Repressive Complex 2 Coordinates Cell Type Proliferation and Differentiation

Miguel de Lucas, Li Pu, Gina Marie Turco, Allie Gaudinier, Ana Karina Marao, Hirofumi Harashima, Dahae Kim, Mily Ron, Keiko Sugimoto, Francois M Roudier and Siobhan M. Brady
Plant Cell; originally published online September 20, 2016;
DOI 10.1105/tpc.15.00744

This information is current as of September 25, 2016

Supplemental Data	http://www.plantcell.org/content/suppl/2016/09/20/tpc.15.00744.DC1.html
Permissions	https://www.copyright.com/ccc/openurl.do?sid=pd_hw1532298X&issn=1532298X&WT.mc_id=pd_hw1532298X
eTOCs	Sign up for eTOCs at: http://www.plantcell.org/cgi/alerts/ctmain
CiteTrack Alerts	Sign up for CiteTrack Alerts at: http://www.plantcell.org/cgi/alerts/ctmain
Subscription Information	Subscription Information for <i>The Plant Cell</i> and <i>Plant Physiology</i> is available at: http://www.aspb.org/publications/subscriptions.cfm